https://doi.org/10.5194/bg-2021-139
Preprint. Discussion started: 4 June 2021

Biogeosciences Discussions

The Cretaceous physiological adaptation of angiosperms to a declining pCO_2 : a trait-oriented modelling approach

Julia Bres[1], Pierre Sepulchre[1], Nicolas Viovy[1], and Nicolas Vuichard[1]

[1]Laboratoire des Sciences du Climat et de l'Environnement, LSCE/IPSL, CEA-CNRS-UVSQ, Université Paris-Saclay, 91191 Gif-sur-Yvette, France

Correspondence: Julia Bres (julia.bres@lsce.ipsl.fr)

Abstract. The Cretaceous evolution of angiosperm leaves towards higher vein densities enables unprecedented leaf stomatal conductance. Still, simulating and quantifying the impact of such change on plant productivity and transpiration in the peculiar environmental conditions of the Cretaceous remains challenging. Here, we address this issue by combining a paleo proxy-based model with a fully atmosphere-vegetation model that couples stomatal conductance to carbon assimilation. Based on the fossil record, we build and evaluate three consistent pre-angiosperm vegetation parameterizations under two end-members scenarios of pCO_2 (280 ppm and 1120 ppm) for the mid-Cretaceous : a reduction of hydraulic or photosynthetic capacity and a combination of both, supported by a likely coevolution of stomatal conductance and photosynthetic biochemistry. Our results suggest that decreasing hydraulic or/and photosynthetic capacities always generates a reduction of transpiration that is predominantly the result of plant productivity variations, modulated by light, water availability in the soil and atmospheric evaporative demand. The high pCO_2 acts as a fertilizer on plant productivity that bolsters plant transpiration and water-use efficiency. However, we show that pre-angiosperm physiology does not allow vegetation to grow under low pCO_2 because of a positive feedback between leaf stomatal conductance and leaf area index. Our modelling approach stresses the need to better represent paleovegetation physiological traits. It also confirms the hypothesis of a likely evolution of angiosperms from a stage of low hydraulic and photosynthetic capacities at high pCO_2 to a stage of high hydraulic and photosynthetic capacities linked to leaves more and more densely irrigated together with a more efficient biochemistry at low pCO_2.

1 Introduction

Vegetation plays a pivotal role in the climate system as it controls water and energy fluxes at the interface between land surfaces and the atmosphere through albedo (Charney et al., 1975; Port et al., 2016; Brovkin et al., 2009), roughness length, and evapotranspiration capabilities (e.g., Bathiany et al., 2010; Betts et al., 1997; Kleidon et al., 2000; Gibbard et al., 2005). Specifically, evapotranspiration (ET), i.e. the sum of soil evaporation, vegetation evaporation and vegetation transpiration fluxes, is a key term in the continental hydrological cycle, and has been shown to control moisture convergence and convection, thereby precipitation patterns in the tropics either in present-day-like configurations (Sun and Barros, 2015; Fraedrich et al., 1999) or for past climates (e.g., Braconnot et al., 1999; Brovkin et al., 2006). It is therefore mandatory that earth system models designed to simulate climate evolution, either in the past or in the future, account for plant traits that alter these fluxes, despite the numerous

https://doi.org/10.5194/bg-2021-139
Preprint. Discussion started: 4 June 2021

challenges involved (Fisher and Koven, 2020). Including vegetation traits in land surface models is a growing field of research (Kattge et al., 2020), but mostly dedicated to better represent present-day vegetation and its response to human-induced climate change (Scheiter et al., 2013; Dury et al., 2018; Peng et al., 2020; Davin and de Noblet-Ducoudré, 2010). The problem has an additional degree of complexity for million-years-old ("deeptime") climates, for which the vegetation physiological traits have been very different from the present. As shown recently for the extinct vegetation of the late Paleozoic, fossil plants provide invaluable information regarding "paleo-traits" that can be in turn included in land surface models (White et al., 2020; Richey et al., 2021).

Another case-study for testing the impact of pivotal changes in physiological traits on the vegetation characteristics is the Cretaceous angiosperm radiation (Boyce and Lee, 2010; Boyce et al., 2010; De Boer et al., 2012). With more than 295,000 species described, angiosperms represent more than 95 % of modern terrestrial vascular plant diversity (Christenhusz and Byng, 2016). One of the most emblematic changes in vegetation through Earth history is their diversification at the expanse of gymnosperms during the Cretaceous (Condamine et al., 2020). The macroflora fossil record reveals significant changes in leaf anatomy between the early Cretaceous and the late Cretaceous associated with the rise of angiosperms. Specifically, measurements on fossil leaves show that vein density (D_v) increased from 3.1 mm mm^{-2} for the oldest angiosperms leaves from the Aptian-Albian (115 Ma) to 9.8 mm mm^{-2} by the Maastrichtian-Paleocene (66 Ma), while gymnosperms D_v remained centered around 2.4 mm mm^{-2} over the same period (Feild et al., 2011a). Contemporaneous changes in stomatal size (S) and density (D_s) are observed in the fossil record (De Boer et al., 2012) showing a strong correlation with vein density. While veins allow the plants to efficiently transport water from the soil close to the site of transpiration i.e stomata, the latter allow the leaves to efficiently exchange carbon and water with the atmosphere. Studies have already shown that D_v is a reliable marker of hydraulic capacity (Brodribb et al., 2007; Brodribb and Feild, 2010; Feild et al., 2011a, b; Boyce et al., 2010; Lee and Boyce, 2010; Boyce et al., 2009; Boyce and Lee, 2010, 2017) and pioneer modelling studies have explored the impact of such a variation of vein density on the transpiration rate in present-day conditions (Boyce et al., 2010; Lee and Boyce, 2010; Boyce and Lee, 2010, 2017). Based on the closed link between vein density, hydraulic and photosynthetic capacities (Brodribb et al., 2007), linear relationships have been inferred between D_v and (1) the transpiration rate on one hand (Boyce et al., 2009; Boyce and Lee, 2017; Boyce et al., 2010), and (2) the maximum rate of carboxylation (V_{cmax}), involved in photosynthesis, on the other hand (Boyce and Lee, 2010; Lee and Boyce, 2010). Sensitivity tests carried out with a land surface model coupled to an atmospheric circulation model showed that angiosperms with modern traits bolster the current hydrological cycle, ensuring seasonally high levels of transpiration and precipitation rates in the tropics (Lee and Boyce, 2010; Boyce and Lee, 2010, 2017; Boyce et al., 2010).

Even if a lot of functional traits evolved during the angiosperm radiation, in this paper we will focus on changes of leaf stomatal conductance and photosynthetic capacity. In particular, since they are highly related to environmental changes, our approach relies on the integration of fossil traits in a land surface model in order to quantify how transpiration and photosynthesis responded to the angiosperm leaf trait evolution in the peculiar environmental conditions of the Cretaceous (different paleogeography and high atmospheric CO_2 concentrations). Land surface models used in climate modelling do not explicitly represent traits such as vein densities but rather directly simulate the operational stomatal conductance at the leaf scale (g_s)

https://doi.org/10.5194/bg-2021-139
Preprint. Discussion started: 4 June 2021


Biogeosciences Discussions Open Access EGU

(Farquhar et al., 1980; Ball et al., 1987; Krinner et al., 2005; Yin and Struik, 2009). However, based on relationships obtained from extant and fossil leaves that links maximal anatomic stomatal conductance to H_2O (g_{anat}^{max}) to D_v (Brodribb et al., 2007; Brodribb and Feild, 2010), they can be parameterized to represent the changes in stomatal conductance that occured with the angiosperm radiation. Depending on the choices made, these parameterizations can reflect changes on plant traits controlling hydraulic capacity, photosynthetic capacity or both. The latter is supported by our knowledge of modern plant processes and in particular of a coevolution between stomatal conductance and V_{cmax} (Franks and Beerling, 2009a; De Boer et al., 2012). Although there is no fossil evidence of changes in photosynthetic capacity, we assume that this covariation is a time-invariant property and that such relationship was the same in the past. Moreover, atmospheric pCO_2 is known to control the degree of stomatal opening and closing at very short-term (Jarvis et al., 1999). Several studies have reported that the g_s/g_{anat}^{max} ratio is relatively stable around 20-40 %, an optimal range within which changes in guard cell turgor pressure are most efficient in controlling quick stomatal conductance changes (Dow et al., 2014; Dow and Bergmann, 2014; McElwain et al., 2016). Therefore, it is likely that pCO_2 also drives changes in g_{anat}^{max} on long time scales. Paleo-CO_2 reconstructions based on proxies (plant fossils and isotopes) and geochemical models show that, despite a large spread, pCO_2 was high throughout the Cretaceous, ranging from 500 ppm to 2000 ppm. Values peaked during the mid-Cretaceous (Cenomanian-Turonian, ca. 95 Ma), then steadily declined towards the Cretaceous-Paleogene boundary (Fletcher et al., 2008; Wang et al., 2014). It is thus important to consider this varying pCO_2 when exploring the mechanisms of the angiosperm physiological changes. Finally, the goal of our study is to evaluate the combined environmental and physiological-induced response of plants evolving higher D_v with a coupled atmosphere-vegetation model. This experimental design considers both reducing plant hydraulic or/and photosynthetic capacities and applying different forcing in pCO_2, allowing the modeled g_s to account for long-term plant adaptation to their changing environment.

2 Methods

2.1 IPSL atmosphere-land surface model

In this study, we use LMDz and ORCHIDEE versions embedded in the IPSL-CM5A2 model (Sepulchre et al., 2020). LMDz is the atmosphere general circulation model of the Institut Pierre-Simon Laplace earth system model. LMDz couples a dynamical core solving the primitive equations of conservation with a set of physical parameterizations of the radiative and convective schemes. The spatial resolution of LMDz is the regular 3.75 x 1.875° longitude-latitude grid. LMDz has 39 vertical levels to describe vertical processes (Hourdin et al., 2013). ORCHIDEE is the land surface component of the IPSL earth system model (Krinner et al., 2005). When coupled with LMDz, it has the same horizontal resolution, and a 4-meter soil water depth represented with a two-layer bucket model. ORCHIDEE simulates water and energy exchanges (Rosnay and Polcher, 1998; Ducoudré et al., 1993), and the key processes of the terrestrial carbon cycle such as photosynthesis, carbon allocation, or soil organic matter decomposition for thirteen Plant Functional Types (PFTs). Each PFT gathers a set of plant species with similar functional characteristics that will be translated into a common set of parameter values. Photosynthesis, water and energy

https://doi.org/10.5194/bg-2021-139
Preprint. Discussion started: 4 June 2021

exchanges are computed every 30 minutes while carbon-related slow processes are computed on a daily basis (Krinner et al., 2005; Sitch et al., 2003).

2.1.1 Stomatal conductance in ORCHIDEE

Stomatal conductance is computed per canopy layer, with layer depth increasing exponentially from top to bottom of the canopy. This feature enables to account for the response to light radiation extinction through the canopy. Leaf stomatal conductance modelling is coupled to photosynthesis based on original formulations from Ball et al. (1987) and Leuning et al. (1995). Within the model used in ORCHIDEE (Yin and Struik, 2009), leaf operational stomatal conductance to H_2O, g_s (mol m^{-2}[leaf] s^{-1}), depends on the net carbon assimilation A (molCO_2 m^{-2}[leaf] s^{-1}), the day respiration R_d (molCO_2 m^{-2}[leaf] s^{-1}), the intercellular CO_2 partial pressure C_i (bar), the C_i-based CO_2 compensation point in the absence of R_d, C_i^* (bar), a factor fcpl, describing the strength of the coupling between A and g_s, which is function of the leaf-to-air vapor pressure deficit and that we will further name "hydraulic capacity", and the residual stomatal conductance to H_2O, g_0 (mol m^{-2}[leaf] s^{-1}) to account for a non-zero conductance when the carbon assimilation is zero (Farquhar et al., 1980; Ball et al., 1987; Yin and Struik, 2009):

$$g_s = g_0 + \frac{A + R_d}{C_i - C_i^\star} * fcpl \tag{1}$$

The semi-empirical formalism of g_s allows to account for both the structural conductance, linked to leaves morphologic and physiologic traits (e.g. D_v, D_s and S) developed on the long-term plant evolution history, and the dynamical conductance, related to the short-term stomatal opening and closing depending on the environment. A is limited by either the Rubisco enzyme (RuBP) activity (V_c) or the electron transport (V_j):

$$A = min(V_c, V_j) \tag{2}$$

V_c represents the ability of the RuBP to fix CO_2 and initiate the Calvin cycle. It relies on V_{cmax}, K_c and K_o the Michaelis-Menten constants of Rubisco for CO_2 and O_2 respectively (bar) and O the oxygen partial pressure (bar):

$$V_c = \left[\frac{(C_i - C_i^\star)V_{cmax}}{C_i + K_c\left(1 + \frac{O}{K_O}\right)} - R_d \right] * \left[1 - w_{soil}^{lim}\right] \tag{3}$$

V_{cmax} is parameterized for each PFT as a function of leaf age (Krinner et al., 2005). V_j represents the regeneration rate of the RuBP. The latter depends on the radiation and the electron transport :

$$V_j = \left[\frac{(C_i - C_i^\star)J}{4C_i + 8C_i^\star} - R_d \right] * \left[1 - w_{soil}^{lim}\right] \tag{4}$$

Where J is the actual rate of electron transport (Yin and Struik, 2009), dependent on irradiance and V_{jmax}, the maximum rate of electron transport at saturating light (mol e- m^{-2} s^{-1}). V_{jmax} is directly proportional to V_{cmax} with the ratio V_{cmax}/V_{jmax} varying with surface monthly temperature (Kattge and Knorr, 2007). Then, when discussing the changes in V_{cmax}, we consider the proportional changes in V_{jmax}, in the following. A increases with V_{cmax} and pCO_2, until to reach a plateau where light

https://doi.org/10.5194/bg-2021-139
Preprint. Discussion started: 4 June 2021


Biogeosciences Discussions Open Access EGU

and temperature become the limiting factors. Both V_c and V_j are a function of the soil moisture stress for transpiration w_{soil}^{lim}, that ultimately controls photosynthesis. This factor depends on both the soil moisture and the root profile given per PFT, trees having deeper roots than grasses. w_{soil}^{lim} is unitless and ranges between 0 for fully moist soil and 1 for maximal water stress. The transpiration rate Tr (mm d^{-1}) is a function of the potential evapotranspiration, that is, the atmospheric evaporative demand, modulated by a serie of resistances :

$$Tr = \frac{1}{r_c + r_a} \rho (q_s^\star - q) \tag{5}$$

where r_a and r_c are the aerodynamic and canopy resistances respectively (s m^{-1}), ρ is the air density (kg m^{-3}), q_s^* is the saturation specific humidity of the evaporating surface (kg kg^{-1}), function of the temperature, and q is the specific humidity of the surrounding air (kg kg^{-1}). Calculation of the transpiration requires the integration of g_s at the canopy level which is g_c (molH_2O m^{-2}[ground] s^{-1}), that is over the leaf area index (LAI) and expressed as :

$$g_c = \int_{l=0}^{l=LAI} g_s(l)\,\mathrm{d}l \tag{6}$$

$$g_c = \frac{1}{r_c} \tag{7}$$

2.1.2 Summary of dynamical coupling between stomatal conductance and photosynthesis in a given environment

At the leaf level, the structural resistance (Fig. 1, in orange) represents traits (veins and stomata) that evolve at long time scales. The structural resistance drives the maximum theoretical conductance of water (g_{anat}^{max}). The dynamical resistance (Fig. 1, in dark blue) controls the stomatal closure on a very short time scale. Plants can also slightly adapt their V_{cmax} and V_{jmax}, in absence of nitrogen stress, on seasonal timescale and in a greater range on evolutionary long time scales. External forcing are pCO_2, light, rainfall, relative humidity, wind stress and soil moisture stress for transpiration (Fig. 1, in light blue). The coupling factor (fcpl) controls the sensitivity of stomatal conductance to the surrounding environment : a low fcpl implies that g_s is less sensitive to C_i, A and the vapor pressure deficit than a high fcpl. The end limit of the assimilation process is the available energy from light that controls the quantity of RuBP that can be regenerated (V_j in Eq. (4)). At high pCO_2, C_i is maintained at a sufficient level to feed the carboxylation rate (V_c) and then, for a sufficient V_{cmax}, light becomes the main limiting factor even for a small conductance (Eq. (2) to (4)). So, the structural resistance is not a limiting factor and plants will close the stomata to limit the water loss. Likewise, V_c rate increases, with both C_i and V_{cmax}, and the level of V_{cmax} for which V_j becomes the main limiting factor decreases (Eq. (2)). Because nitrogen acquisition and RuBP protein maintenance are highly energetic for the plants, they tend to optimize the V_{cmax} and V_{jmax} to reach the point where V_c and V_j are colimiting (Maire et al., 2012). On the contrary, at low pCO_2 structural conductance (that drives the maximum conductance) can become a limiting factor since, even with full stomata opening, it can limit C_i under the level to feed the carboxylation rate. V_{cmax} and V_{jmax} should also be increased to maintain a sufficient level of carboxylation (V_c) (lower efficiency of the oxidation/carboxylation ratio).

https://doi.org/10.5194/bg-2021-139
Preprint. Discussion started: 4 June 2021

Biogeosciences
Discussions
Open Access
EGU

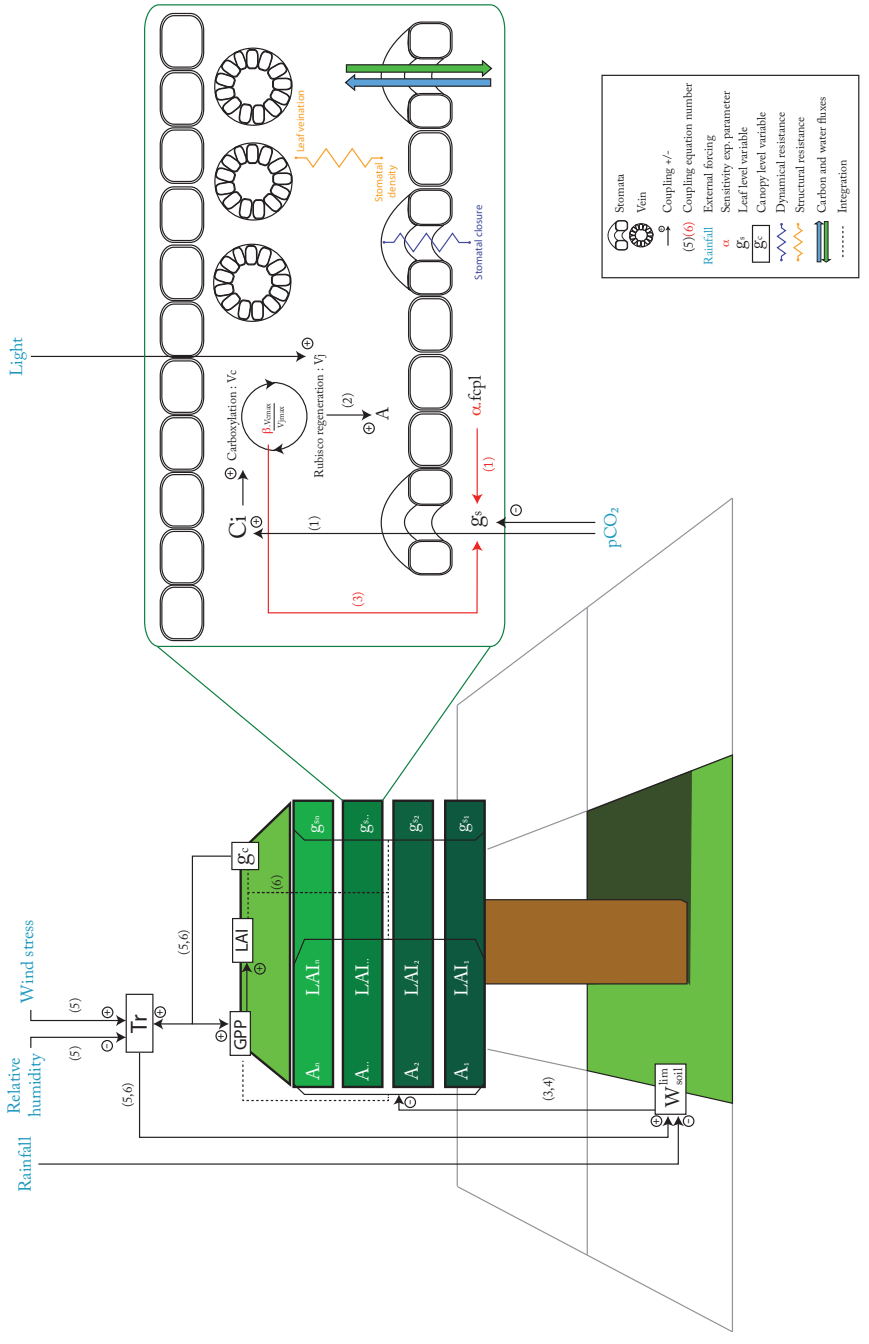

Figure 1. Schematized coupling between stomatal conductance and photosynthesis from the leaf to the canopy scale in the ORCHIDEE model.

At the canopy level (Fig. 1), the canopy conductance g_c depends on both leaf level conductance g_s and LAI. As LAI is a function of plant productivity, there is an additional positive feedback: a change in g_s will impact GPP and then LAI in the

https://doi.org/10.5194/bg-2021-139
Preprint. Discussion started: 4 June 2021

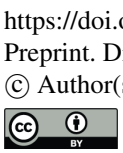

same direction, which will amplify the initial effect of g_s on g_c. Another external forcing is the soil water availability (w_{soil}^{lim}). A low soil water content will induce a water stress limiting the V_{cmax} and V_{jmax} that will indirectly also reduce g_s. Hence, arid ecosystems will be less sensitive to structural change in g_s than ecosystems without a large hydric stress. On the contrary, they will be affected in the same way for direct changes on V_{cmax} and V_{jmax}.

2.2 Fossil evidence of increasing angiosperm hydraulic and photosynthetic capacities

Vein density as well as stomatal size and density are both used to reconstruct past variations of g_{anat}^{max} (Franks and Beerling, 2009a, b; Brodribb et al., 2007; Brodribb and Feild, 2010; De Boer et al., 2012; Franks and Farquhar, 2001). Here, we have chosen to account for D_v changes rather than D_s and S. Indeed, using D_v is a good proxy to constrain g_{anat}^{max} since D_v and D_s are correlated and that observed relationship between D_v and g_{anat}^{max} gives the highest correlation coefficient (Feild et al., 2011b). Vein densities from angiosperm fossils published in Feild et al. (2011b) record a 2 to 5-fold increase in angiosperm D_v during the Cretaceous (Fig. 2a), compared to early angiosperms and non-angiosperm (Table S1).

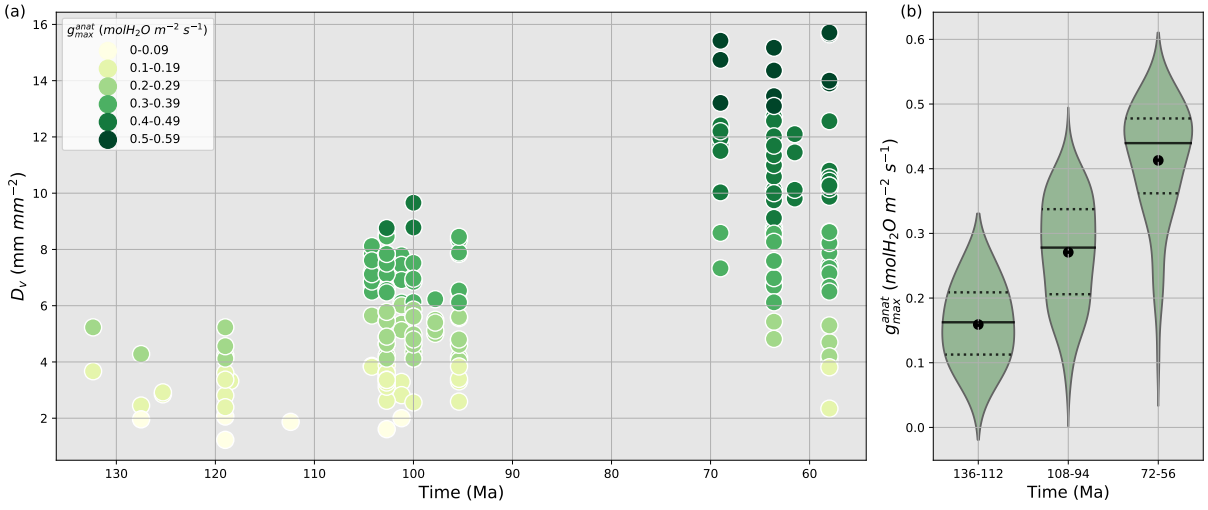

Figure 2. (a) Time evolution of fossil vein densities (mm mm^{-2}, y-axis) adapted from Feild et al. (2011a) and the corresponding maximal stomatal conductance to H_2O (mol m^{-2} s^{-1}, filled circles) calculated by the anatomic relationship developed by Brodribb et al. (2007) and Brodribb and Feild (2010). (b) Subdivision of maximal stomatal conductance to H_2O (mol m^{-2} s^{-1}) by time periods. The solid line is the median, the dotted lines are the first and third quartiles, and the point is the mean value for each time period.

D_v allows to reconstruct the maximal water that can flow through the stomata g_{anat}^{max} (mol m^{-2} s^{-1}) using the relationship developed by Brodribb et al. (2007) and Brodribb and Feild (2010) :

$$g_{max}^{anat} = \frac{12760}{\nu}\Delta\Psi_{leaf}\left(\frac{\pi}{2}\sqrt{\frac{650^2}{D_v^2}+y^2}\right)^{-1.27} \quad (8)$$

Where ν is the leaf-to-air vapor pressure deficit (MPa), $\Delta\Psi_{leaf}$ is the leaf water potential gradient (MPa), D_v is the vein density (mm mm^{-2}) and y is the distance from vein terminals to epidermis (μm). ν and $\Delta\Psi_{leaf}$ are set to 0.002 MPa and

https://doi.org/10.5194/bg-2021-139
Preprint. Discussion started: 4 June 2021

0.4 MPa respectively, values that are typical for temperate-tropical environments (Brodribb and Feild, 2010). An estimation of y is 70-130 μm, producing a span of predicted values encompassing the likely morphological variability of leaves (Brodribb and Feild, 2010). The lower y is, the closer the vein is to the stomata and the higher g_{anat}^{max} is. The highest increase in g_{anat}^{max} is obtained for the largest variation of D_v over time combined with the smallest y. Conversely, the lowest increase in g_{anat}^{max} is obtained for the smallest variation of the highest D_v values over time, combined with the highest y (Table S1). From the early to the late Cretaceous, the 2 to 5-fold increase in angiosperm D_v corresponds to a 3 to 5-fold increase in g_{anat}^{max} (Fig. 2b and Table S1). Thus, fossil D_v provides an estimation of the increase in g_{anat}^{max} over time. Our land surface model does not explicitly represent vegetation traits nor g_{anat}^{max} but only g_s, the operational stomatal conductance. However, based on the strong relationship between g_{anat}^{max} and g_s (Dow et al., 2014; Dow and Bergmann, 2014), one assumes that variations of g_s due to the long-term evolution of hydraulic and photosynthetic capacities together with that of environmental factors such as pCO_2 would reflect into proportional changes on g_{anat}^{max}.

2.3 Experimental setup

To assess the impact of angiosperm leaf evolution on transpiration and photosynthesis, we performed climate model simulations while varying plant hydraulic or photosynthetic capacity, or both for two contrasted pCO_2 levels (Table 1). The model continental boundary conditions include mid-Cretaceous (115 Ma) paleogeography reconstructions from Sewall et al. (2007). Global vegetation distribution (Fig. 3) is set by establishing a first-order estimate of correspondence between biomes, inferred from paleobotanical data (Sewall et al., 2007), and PFTs (Table S2).

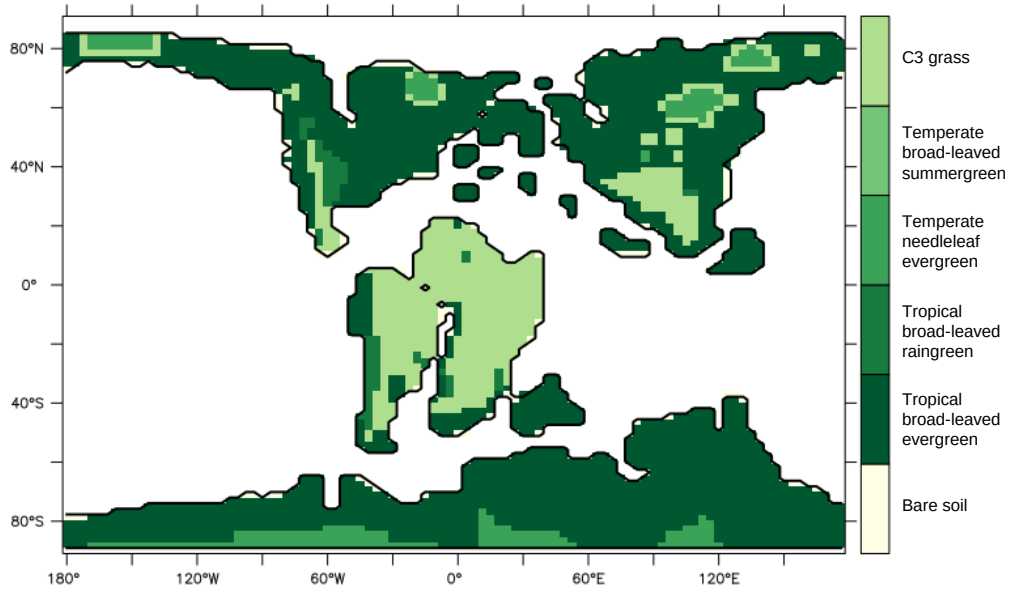

Figure 3. Vegetation distribution in the Aptian simulation configuration : map showing the dominant PFT for each grid cell. For all experiments, this distribution is fixed along the time.

https://doi.org/10.5194/bg-2021-139
Preprint. Discussion started: 4 June 2021

This configuration allows the carbon cycle to be activated and the LAI to be prognostically calculated as a function of dynamic carbon allocation (Krinner et al., 2005). We set the solar radiation at 99 % of the current value and the orbitals parameters as today. The ocean is prescribed through sea-surface temperatures obtained from an unpublished Aptian fully-coupled simulation obtained with the ESM IPSL-CM5A2 (Sepulchre et al., 2020). To assess the impact of angiosperm trait evolution on transpiration and photosynthesis, we consider (i) two different parameters applied to angiosperm-PFTs only, and (ii) one external forcing (pCO_2), that alter the stomata conductance in our land-surface model (Table 1).

Table 1. Definition of the experiments

Name	Parameters representing the fraction of current plant capacities for angiosperms PFTs		pCO_2 (ppm)	Description
	Hydraulic capacity (α)	Photosynthetic capacity (β)		
ANGIO(1120)	1	1	1120	Cretaceous world with the high hydraulic and photosynthetic capacities of modern angiosperms
NOANGIOh(1120)	$1/5$	1	1120	Cretaceous world without the high hydraulic capacity of modern angiosperms
NOANGIOp(1120)	1	$1/5$	1120	Cretaceous world without the high photosynthetic capacity of modern angiosperms
NOANGIOhp(1120)	$\sqrt{1/5}$	$\sqrt{1/5}$	1120	Cretaceous world without the high hydraulic and photosynthetic capacities of modern angiosperms
ANGIO(280)	1	1	280	Cretaceous world with the high hydraulic and photosynthetic capacities of modern angiosperms, under preindustrial pCO_2
NOANGIOh(280)	$1/5$	1	280	Cretaceous world without the high hydraulic capacity of modern angiosperms, under preindustrial pCO_2
NOANGIOp(280)	1	$1/5$	280	Cretaceous world without the high photosynthetic capacity of modern angiosperms, under preindustrial pCO_2
NOANGIOhp(280)	$\sqrt{1/5}$	$\sqrt{1/5}$	280	Cretaceous world without the high hydraulic and photosynthetic capacities of modern angiosperms, under preindustrial pCO_2

https://doi.org/10.5194/bg-2021-139
Preprint. Discussion started: 4 June 2021


Biogeosciences Discussions Open Access EGU

Changes in hydraulic capacity is considered via a change in the coupling factor (fcpl) that describes the slope of the relationship between g_s and the dynamical driving parameters (namely A, pCO_2 and vapor pressure deficit). Because fcpl is related to the structural conductance, the change in g_{anat}^{max} can then be empirically represented by a parameter α, modulating fcpl in the g_s formulation (Eq. (1)). Changes in photosynthetic capacity are taken into account via changes in V_{cmax}/V_{jmax} ratio (Eq. (2) to (4)). To this end, we use a parameter β that acts directly on V_{cmax} (Eq. (3)). We carry out three different factorial experiments using the upper value of changes in g_{anat}^{max} induced from D_v proxy as depicted earlier. (1) α is set to $1/5$ while β is 1, accounting for a direct decrease of flowering plant hydraulic capacity by a factor of 5 (NOANGIOh, Table 1). (2) β is set to $1/5$ while α is 1, corresponding to a direct decrease of angiosperm photosynthetic capacity by a factor of 5 (NOANGIOp, Table 1). This sensitivity experiment is supported by the coupling between stomatal conductance and assimilation in the model and by several studies suggested to mimic pre-angiosperm capacities by decreasing modern V_{cmax} by a factor of 5 (Boyce and Lee, 2010; Lee and Boyce, 2010). Since plant hydraulic and photosynthetic capacities are likely to have co-evolved over the Cretaceous (Franks and Beerling, 2009a; De Boer et al., 2012), (3) we set α and β to $\sqrt{1/5}$, i.e with half the forcing simultaneously applied to the hydraulic and the photosynthetic capacities (NOANGIOhp, Table 1). These three sensitivity tests model three likely Cretaceous worlds without modern-like angiosperms. We perform an additional experiment where the parameters α and β are set to 1 in order to keep the modern hydraulic and photosynthetic capacity of extant angiosperms (ANGIO, Table 1). Since pCO_2 simultaneously impacts hydraulic and photosynthetic traits evolution on the long-term (Franks and Beerling, 2009a), we repeat this set of experiments for two different extreme pCO_2 forcings. At 1120 ppm, we refer to the mid-Cretaceous (115 Ma) estimates, contemporary with the beginning of the angiosperm radiation. At 280 ppm, we make a sensitivity test to assess the response of pre-angiosperm vegetation to a preindustrial-like pCO_2. Assuming the g_s/g_{anat}^{max} ratio is a constant at long-time scales because of plants structural adaptation to their environment, we consider that all the changes in the model operational g_s arising from the above-mentioned pre-angiosperm parameterizations reflect that of the maximal anatomic stomatal conductance. The experiments were run for 60 years, a sufficient time to balance gross primary productivity and evapotranspiration. We analyse and show the averaged last 10 years of simulations.

3 Results

The leaf stomatal conductance to H_2O (g_s, mol m^{-2}[leaf] s^{-1}) is given by a unit of foliar surface where exposure to sunlight is maximal. Figure 4 shows that leaf stomatal conductance decreases as we sequentially reduce hydraulic (NOANGIOh) or photosynthetic (NOANGIOp) capacities, or both (NOANGIOhp), to mimic the pre-angiosperm world. Reducing the high hydraulic and/or photosynthetic capacities from modern angiosperm leads to a 3-time drop of leaf stomatal conductance on average, a factor in the lowest bracket of the range expected from g_{anat}^{max} inferred from the fossil record (Fig. 2b). Within every PFT group, g_s decrease is similar amongst sensitivity experiments and validates our chosen combinations of values for α and β. The maximal decrease in g_s is simulated for the tropical broad-leaved evergreen and the C3 grass PFTs which also depict the largest stomatal conductance in the reference ANGIO simulations. Hydraulic and photosynthetic parameters have not been altered for the temperate needleleaf evergreen PFT, as they correspond to gymnosperms. Thus, gymnosperm g_s was expected

https://doi.org/10.5194/bg-2021-139
Preprint. Discussion started: 4 June 2021

to be constant for each of the pCO_2 group of experiments. However, g_s slightly decreases in the sensitivity experiments for this PFT, suggesting a feedback from the atmosphere-vegetation coupling that ultimately altered soil moisture stress and stomatal conductance.

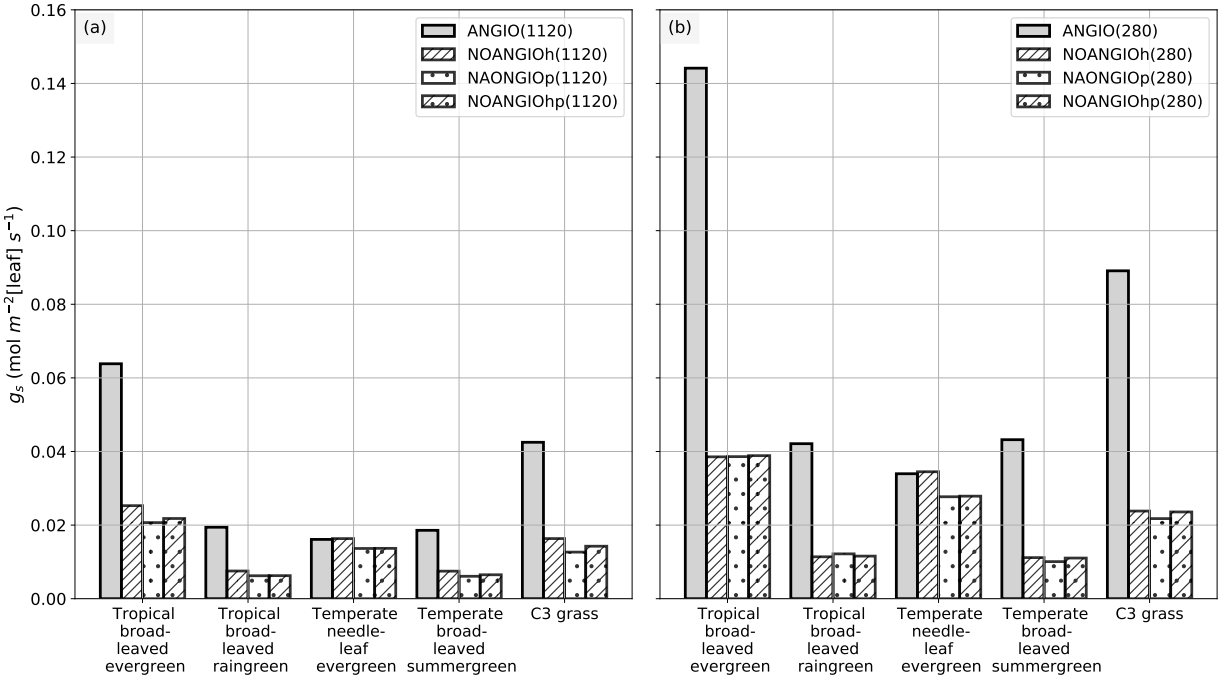

Figure 4. Leaf stomatal conductance to H_2O g_s (mol m^{-2}[leaf] s^{-1}) per PFT : (a) ANGIO(1120) (gray bar), NOANGIOh(1120) (diagonal hatched bar), NOANGIOp(1120) (dotted bar), and NOANGIOhp(1120) (diagonal hatched and dotted bar); (b) ANGIO(280) (gray bar), NOANGIOh(280) (diagonal hatched bar), NOANGIOp(280) (dotted bar), and NOANGIOhp(280) (diagonal hatched and dotted bar). The leaf stomatal conductance to H_2O is the daylight average over the year and the surface grid where each PFT is found.

Simulations forced with "Cretaceous-like" pCO_2 (1120 ppm) show systematically lower g_s values than simulations with pCO_2 set at preindustrial (280 ppm). This illustrates the model reproducing the expected closure of stomata as a response to high pCO_2, in direct link with Eq. (3) and (4). This decrease in g_s with increasing pCO_2 is the highest (52 % on average) for experiments with the modern-like photosynthetic and hydraulic capacities (ANGIO(1120) versus ANGIO(280)). For these experiments, tropical broad-leaved evergreen PFT reacts to the high pCO_2 with g_s values dropping from 0.14 mol m^{-2}[leaf] s^{-1} at 280 ppm to 0.06 mol m^{-2}[leaf] s^{-1} at 1120 ppm, while that of C3 grasses drops from 0.09 to 0.04 mol m^{-2}[leaf] s^{-1}. At 1120 ppm, as the leaf stomatal conductance of ANGIO runs is already strongly reduced compared to that at 280 ppm, the relative decrease in g_s when modern hydraulic and photosynthetic capacities are reduced is also less important : - 66 % for tropical broad-leaved evergreen at 1120 ppm to be compared to -73 % for the same PFT at 280 ppm (Fig. 4).

https://doi.org/10.5194/bg-2021-139
Preprint. Discussion started: 4 June 2021

Annual mean leaf area index (LAI) provides an indication of the vegetation ability to grow given the prescribed boundary conditions, i.e. Cretaceous paleogeography, varying pCO_2 and interactions with the atmosphere. For the modern-like vegetation (ANGIO), figures 5a and b show that the highest LAI values are simulated for regions dominated by tropical broad-leaved evergreen, that are set in mid-to-high latitudes in the peculiar Cretaceous configuration (Fig. 3). LAI is also slightly higher at 1120 ppm than at 280 ppm, as a response to CO_2 fertilization effect on photosynthesis that increases biomass production (Fig. 1). The vegetation response to the prescribed perturbations of fcpl and V_{cmax} strongly differs depending on the pCO_2. At high pCO_2, LAI is unchanged with the sole perturbation of the hydraulic capacity (fcpl$*1/5$, NOANGIOh, Fig. 5c) meaning that even with a reduced g_s at the leaf level, the high pCO_2 allows for the fertilization effect to drive biomass growing (C_i in Eq. (1)). Conversely, V_{cmax} perturbation (NOANGIOp, Fig. 5e) induces a strong decrease in the vegetation cover of all angiosperm PFTs, with LAI dropping to values ranging from 1 to 4 m^2[leaf] m^{-2}[ground] compared to LAI ranging from 1 to 8 m^2[leaf] m^{-2}[ground] for ANGIO(1120). Lastly, when both fcpl and V_{cmax} perturbations are combined (fcpl$*\sqrt{1/5}$ and $V_{cmax}*\sqrt{1/5}$, NOANGIOhp, Fig. 5g), LAI is mostly unchanged, suggesting that in a high pCO_2 context, slightly reduced hydraulic and photosynthetic capacities do not affect actual assimilation. At high pCO_2, the impact of reducing V_{cmax} on photosynthesis is limited because the limiting factor is likely V_j (and then light) rather than V_c (and C_i) (Eq. (2)). At low pCO_2, LAI depicts a much stronger response to perturbations. Reducing the hydraulic capacity leads to a global drop of the vegetation cover, with grass-dominated regions averaging 1 m^2[leaf] m^{-2}[ground] and tree-dominated regions barely reaching 5 m^2[leaf] m^{-2}[ground] except in the very southern latitudes, where no significant change is simulated (Fig. 5d). The strongest signal occurs with the reduction of photosynthetic capacity through V_{cmax} (NOANGIOp, Fig. 5f). Apart from the unchanged needleleaf PFT, the modified vegetation cannot grow in NOANGIOp experiment at 280 ppm, as shown by LAI values close to zero for every angiosperm PFTs. Simulated LAI in NOANGIOhp shows that at a lower V_{cmax} associated with a lower fcpl, tropical PFTs also globally collapse, although vegetation is maintained at high latitude (Fig. 5h). At 280 ppm, intercellular CO_2 partial pressure (Eq. (1) to (4)) becomes more limiting than the solar energy whatever the vegetation prescribed. The latitudinal gradient of LAI reduction testifies to another limiting factor to be integrated, which plays at low latitudes but not at high latitudes. Figure S1b shows that the soil moisture stress for transpiration (Fig. 1, Eq. (3) and (4)) is larger in the tropics to mid-latitudes and near zero at high latitudes. Water in the soil available for transpiration is thus a limiting factor of plant growth in the tropics and mid-latitudes at low pCO_2.

https://doi.org/10.5194/bg-2021-139
Preprint. Discussion started: 4 June 2021

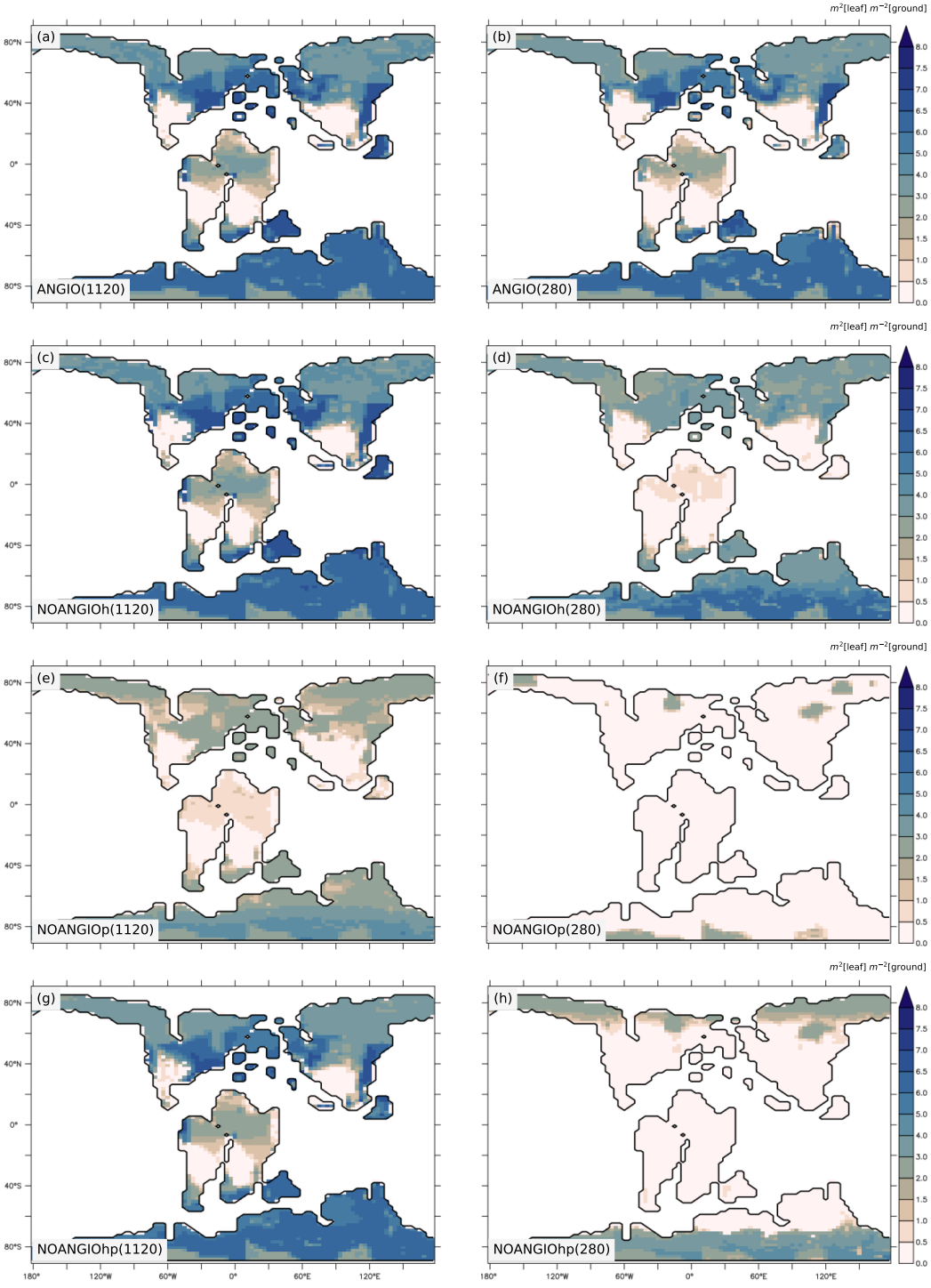

Figure 5. Annual mean LAI (m^2[leaf] m^{-2}[ground]) for (a) ANGIO(1120), (b) ANGIO(280), (c) NOANGIOh(1120), (d) NOANGIOh(280), (e) NOANGIOp(1120), (f) NOANGIOp(280), (g) NOANGIOhp(1120) and (h) NOANGIOhp(280).

https://doi.org/10.5194/bg-2021-139
Preprint. Discussion started: 4 June 2021

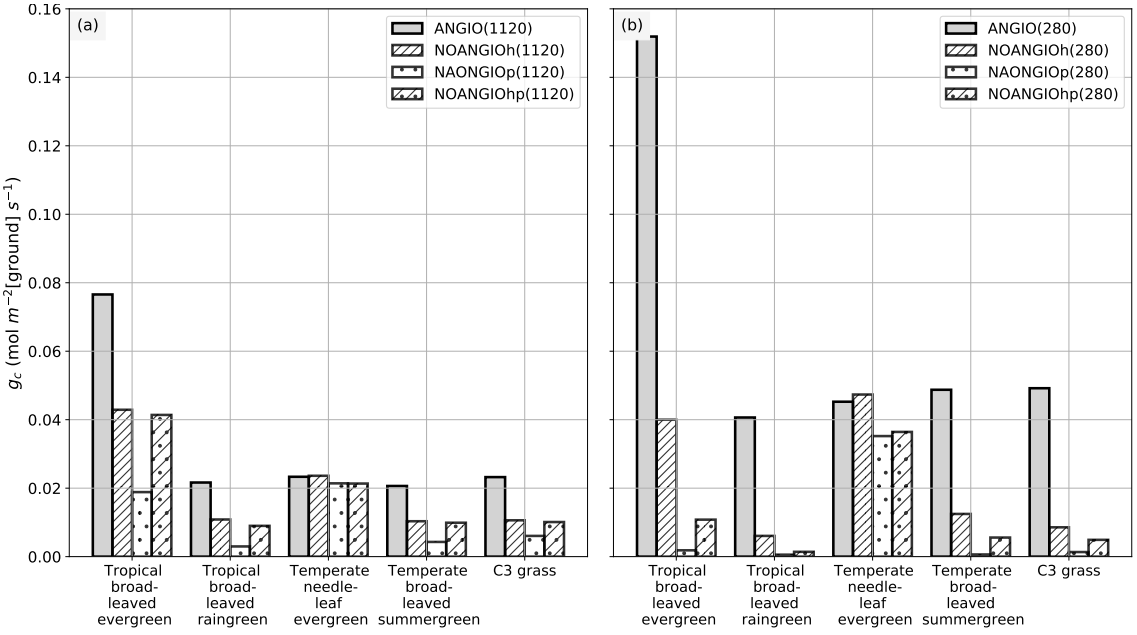

Figure 6. The canopy stomatal conductance to H_2O, g_c (mol m^{-2}[ground] s^{-1}) per PFT : (a) ANGIO(1120) (gray bar), NOANGIOh(1120) (diagonal hatched bar), NOANGIOp(1120) (dotted bar), and NOANGIOhp(1120) (diagonal hatched and dotted bar); (b) ANGIO(280) (gray bar), NOANGIOh(280) (diagonal hatched bar), NOANGIOp(280) (dotted bar), and NOANGIOhp(280) (diagonal hatched and dotted bar). The canopy stomatal conductance to H_2O is the daylight average over the year and the surface grid where each PFT is found.

Albeit the fossil record and empirical models can help to infer the foliar maximal stomatal conductance to H_2O, the land surface model is required to explore the stomatal conductance to H_2O at the canopy level that is given by Eq. (6) and (7): g_c is inversely proportional to the canopy resistance r_c. The canopy stomatal conductance is given by surface unit of ground and integrates the stomatal conductance for shadow leaves at the bottom and sunny leaves at the top of the canopy. Figures 4 and 6 show significant differences between g_s and g_c in respect to the pCO_2 prescribed: while g_s decreases by a factor of 3 for each pre-angiosperm sensitivity experiment compared to the reference (Fig. 4), the decrease in g_c is not equal through experiments (Fig. 6). The dramatic drop in g_c when reducing the high photosynthetic capacity (NOANGIOp) is well explained by the significant LAI decrease (Fig. 5e and f). Besides, the effect of pCO_2 is more complex at the canopy scale. Indeed, g_c is still reduced in the perturbed experiments, but is not systematically lower at 1120 ppm than at 280 ppm (Fig. 6) as opposed to g_s (Fig. 4). NOANGIOh simulations do not show a change in g_c between 280 ppm and 1120 ppm. A decrease in fcpl by a factor of 5 implies a reduction of the LAI at 280 ppm (Fig. 5d) because plants cannot assimilate enough carbon to sustain their biomass (C_i in Eq. (1) to (4)) whereas it is not the case at 1120 ppm (Fig. 5c). Indeed, at the canopy scale, the closing of the stomata at high pCO_2 is compensated by the decrease in LAI at low pCO_2. In the NOANGIOp and NOANGIOhp experiments, g_c is higher at 1120 ppm than at 280 ppm. By increasing the carbon assimilation during photosynthesis (Eq. (1)), high pCO_2 allows for higher vegetation cover (Fig. 5e and g) and higher canopy stomatal conductance whereas low pCO_2 together with low photosynthetic capacity imply a collapse of the vegetation (Fig. 5f and h).

https://doi.org/10.5194/bg-2021-139
Preprint. Discussion started: 4 June 2021


Biogeosciences Discussions Open Access EGU

LAI changes described earlier act as a feedback between g_s and g_c (Fig. 1). At low pCO_2, the LAI decrease between the ANGIO and any of the three perturbed experiments (Fig. 5d, f and h) strengthens the initial decrease in g_s (positive feedback, Fig. 4b and 6b). Mean g_s decreases by 69 %, 73 % and 69 % while mean g_c decreases by 72 %, 97 % and 91 % respectively for NOANGIOh, NOANGIOp and NOANGIOhp compared to ANGIO (Fig. 4b and 6b). Indeed, decreasing V_{cmax} under low pCO_2 implies a reduction of the plant capacity to assimilate carbon (Eq. (3)) and directly impacts the GPP (Fig. in S2f and h) and then the LAI at the canopy scale (Fig. 5f and h). However, decreasing fcpl and thus g_s reduce the CO_2 concentration at the chloroplast level (C_i in Eq. (1)) and have only an indirect effect on GPP (Fig. S2d) and thus on LAI (Fig. 5d). At high pCO_2, the LAI is almost sustained for NOANGIOh and NOANGIOhp compared to ANGIO (Fig. 5a, c and g) because the assimilation remains high when C_i is not the limiting factor (Fig. S2a, c and g). The latter lessens the initial decrease in g_s (Fig. 6a) on g_c (Fig. 4a). Nevertheless, NOANGIOp(1120) experiment shows a much lower g_c than the two previous experiments because of the direct impact of decreasing V_{cmax} on the LAI (Fig. 5e). Therefore, comparing g_c of perturbed simulations to that of the reference allows us to account for the structural conductance linked to plant trait evolution at the canopy level.

As shown in Eq. (5), transpiration rate is controlled by (i) the atmospheric evaporative demand, that depends on air humidity, the surface temperature as well as the aerodynamic resistance, and (ii) the capacity of plants to transpire, driven by the canopy conductance. For both pCO_2 cases, experiments with modern-like vegetation depict the highest transpiration rates in the tropics and the mid-latitudes, where they reach up to 2.5 and 3 mm day^{-1} at 1120 and 280 ppm, respectively (Fig. 7a and b). These regions have optimal conditions in water availability in the soil (Fig. S1b) and light, resulting in higher canopy stomatal conductance (Fig. S3a and b) together with a high atmospheric evaporative demand (Fig. S4a and b) as a response to high temperatures. Transpiration is also slightly strengthened (+ 0.2 mm day^{-1}) at low pCO_2 compared to high pCO_2 (Fig. 7a and b) as a consequence of higher g_c (Fig. 4 and 6).

Parameterizing the vegetation without the modern angiosperms hydraulic and photosynthetic capacities systematically leads to lower transpiration rates (Fig. 7). Overall, in line with changes depicted for LAI and g_c, transpiration rates react stronger in a 280 ppm world than in a 1120 ppm world to decreasing hydraulic and photosynthetic capacities. At 280 ppm, NOANGIOh shows a decrease of 0.6 mm d^{-1} (- 44 %) in transpiration compared to ANGIO, especially over equatorial Gondwana and paleo Southeast Asia, whereas the decrease is limited to 0.3 mm d^{-1} (- 24 %) at 1120 ppm (Fig. 7c and d) as a response to g_c changes described earlier (Fig. 6). Transpiration also significantly drops when photosynthetic capacity alone is reduced (NOANGIOp, Fig. 7e and f). At 1120 ppm, transpiration drops by 0.5 mm d^{-1} (-53 %) (Fig. 7e). The signal is stronger at 280 ppm, where a complete collapse of transpiration is simulated (Fig. 7f). This latter result is a direct consequence of the LAI collapse described earlier (Fig. 5e and f). Combining reduction in photosynthetic and hydraulic capacities (NOANGIOhp) leads to little decreases in transpiration rate at 1120 ppm (Fig. 7g), comparable to NOANGIOh (Fig. 7c), because the high pCO_2 prevents the decrease in carbon assimilation (Fig. 5g) and canopy stomatal conductance (Fig. 6). Conversely, at low pCO_2, the limitation of C_i (Eq. (1), (3) and (4)) implies a collapse of LAI (Fig. 5h) and g_c (Fig. 6) over the tropics and mid-latitudes, and transpiration is near zero for NOANGIOhp, with a decrease of 1 mm d^{-1} (- 81 %) compared to ANGIO (Fig. 7h).

https://doi.org/10.5194/bg-2021-139
Preprint. Discussion started: 4 June 2021

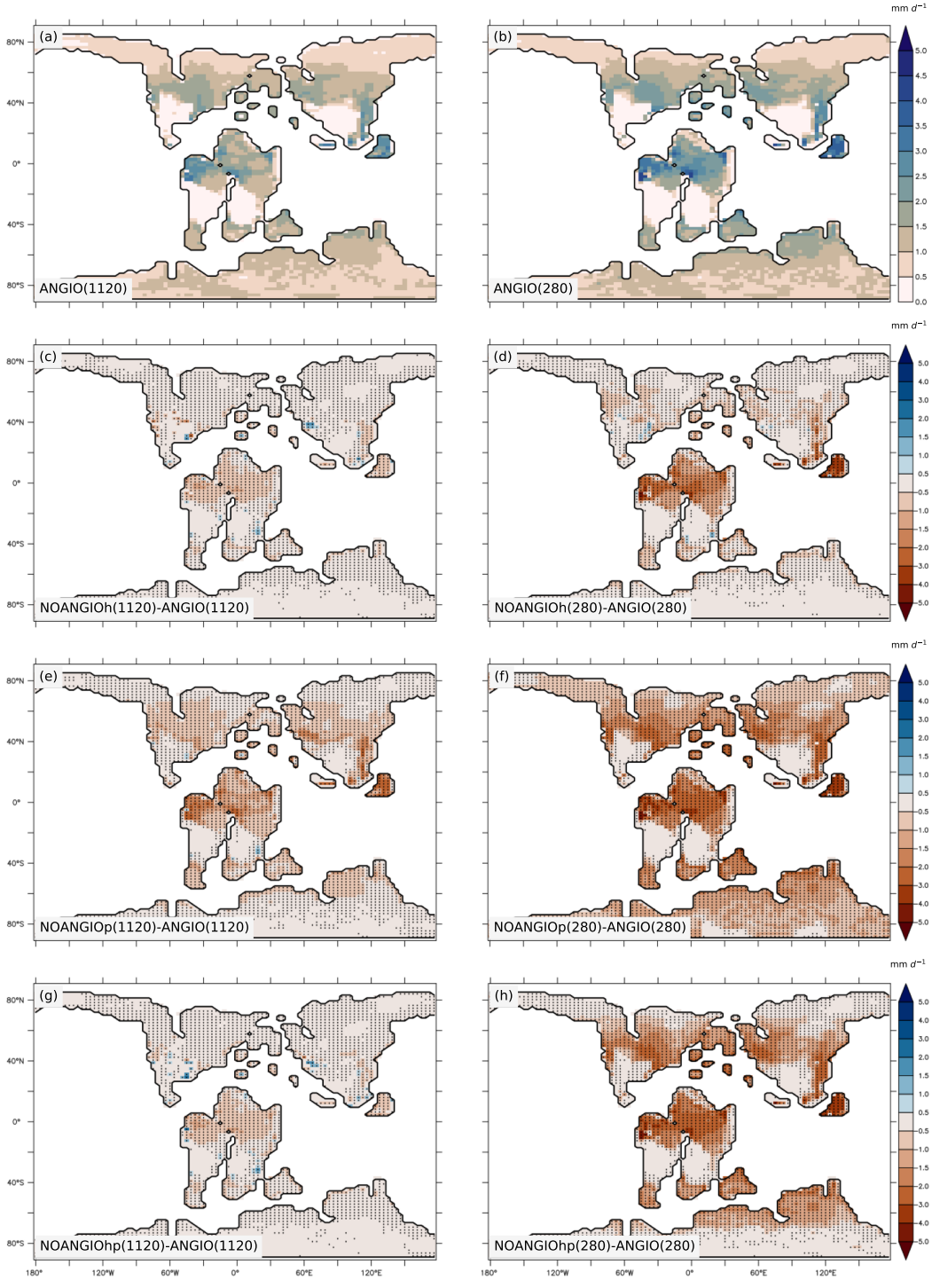

Figure 7. Annual mean transpiration rate (mm d^{-1}) for (a) ANGIO(1120) and (b) ANGIO(280), anomalies of annual mean transpiration rate (mm d^{-1}) for (c) NOANGIOh(1120) vs ANGIO(1120), (d) NOANGIOh(280) vs ANGIO(280), (e) NOANGIOp(1120) vs ANGIO(1120), (f) NOANGIOp(280) vs ANGIO(280), (g) NOANGIOhp(1120) vs ANGIO(1120) and (h) NOANGIOhp(280) vs ANGIO(280). The t-test 95 % confidence level anomalies are given by dots.

https://doi.org/10.5194/bg-2021-139
Preprint. Discussion started: 4 June 2021

Transpiration anomalies come from variations in the atmospheric evaporative demand (Fig. S4) combined with that of the canopy stomatal conductance (Fig. S3), arising from g_s and LAI changes which are modulated by the soil moisture stress for transpiration and light. Transpiration anomalies are located over the paleo-tropics (Fig. 7c and d) for NOANGIOh compared to ANGIO experiments because decreasing hydraulic capacity by a factor of 5 acts mainly on wet regions where plants efficiently transpire in the ANGIO world (Fig. 1 and Eq. (1) to (4)), while arid belt regions are less sensitive to any change in g_c. However, mid-latitude do not show transpiration anomalies because the decrease in g_c (Fig. 6, S3c and d) is compensated by the increase in atmospheric evaporative demand (Fig. S4c and d) that bolsters transpiration rate. In contrast, decreasing photosynthetic capacity (NAONGIOp) acts more globally on terrestrial plants and explains the widespread transpiration anomalies (Fig. 7e and f), always modulated by the atmospheric evaporative demand (Fig. S4e and f). At 1120 ppm, NOANGIOhp shows the same pattern as NOANGIOh (Fig. 7c and g) because plants are more sensitive to reduction in fcpl than to reduction in V_{cmax} (C_i is not limiting) while the decrease in transpiration is more extended at 280 ppm (Fig. 7h) because it arises mainly from the decrease of V_{cmax} at low pCO_2 that drives carbon assimilation to decline (Eq. (2) and (3)).

The annual mean water use efficiency (WUE) is the ratio of annual mean GPP to annual mean transpiration over each grid point (gC kgH_2O^{-1}). It pictures the capacity of vegetation to maximise carbon uptake while minimizing water loss and thus is a good indicator of plants adaptation to their environment. For the modern-like vegetation (ANGIO), maximal values of WUE are found in the mid to high-latitudes where optimal conditions of water and light (Fig. 8a and b, Fig. S1b) are available for the vegetation. WUE increases with pCO_2 : while it barely exceeds 10 gC kgH_2O^{-1} at 280 ppm, it reaches more than 15 gC kgH_2O^{-1} at 1120 ppm. This is explained by the CO_2 fertilization effect generated by the high pCO_2 on C_i (Eq. (2) to (4)) that strengthens plant productivity. At 1120 ppm, the highest value of WUE is found for NAONGIOh, with a 1.7 gC kgH_2O^{-1} (+ 30 %) increase compared to ANGIO (Fig. 8a and c). Indeed, reducing the hydraulic capacity does not imply a change in GPP which remains similar to that of ANGIO(1120) (Fig. S2a and c) but rather generates a slight decrease in transpiration rate (Fig. 7c), explaining the increase of WUE. Therefore, plants with lower hydraulic capacities than today are better adapted to the high pCO_2 environment. For NOANGIOhp(1120), the WUE is partly reduced compared to ANGIO(1120) but stays at a high level (Fig. 8a and g). It results from the larger decrease in GPP than in transpiration rate (Fig. S2g and 7g), as GPP is more sensitive to the V_{cmax} reduction (Eq. (2)) than transpiration is to the fcpl reduction (Eq. (1) and (5)). In contrast, WUE is largely degraded in NOANGIOp(1120) compared to ANGIO(1120) (Fig, 8a and e). Both GPP (Fig. S2a and e) and transpiration rate (Fig. 7a and e) significantly drop when reducing photosynthetic capacity (NOANGIOp) at high pCO_2. However, V_{cmax} acts directly on the carbon assimilation (Eq. (2) and (3)) while it is more indirect on the stomatal conductance, thus implying that the reduction of V_{cmax} has a larger effect on GPP than on transpiration rate. In contrast to experiments at high pCO_2, ANGIO(280) gives the highest WUE at low pCO_2. NOANGIOh(280) depicts a lower WUE than ANGIO(280) (Fig. 8b and d) which demonstrates that plants with lower hydraulic capacity than today are less adapted to the low pCO_2 environment. At low pCO_2, the low C_i decreases GPP (Eq. (3), Fig. S2b and d) while it increases g_s (Eq. (1), Fig. 4), modulating the transpiration decrease (Fig. 7d).

https://doi.org/10.5194/bg-2021-139
Preprint. Discussion started: 4 June 2021

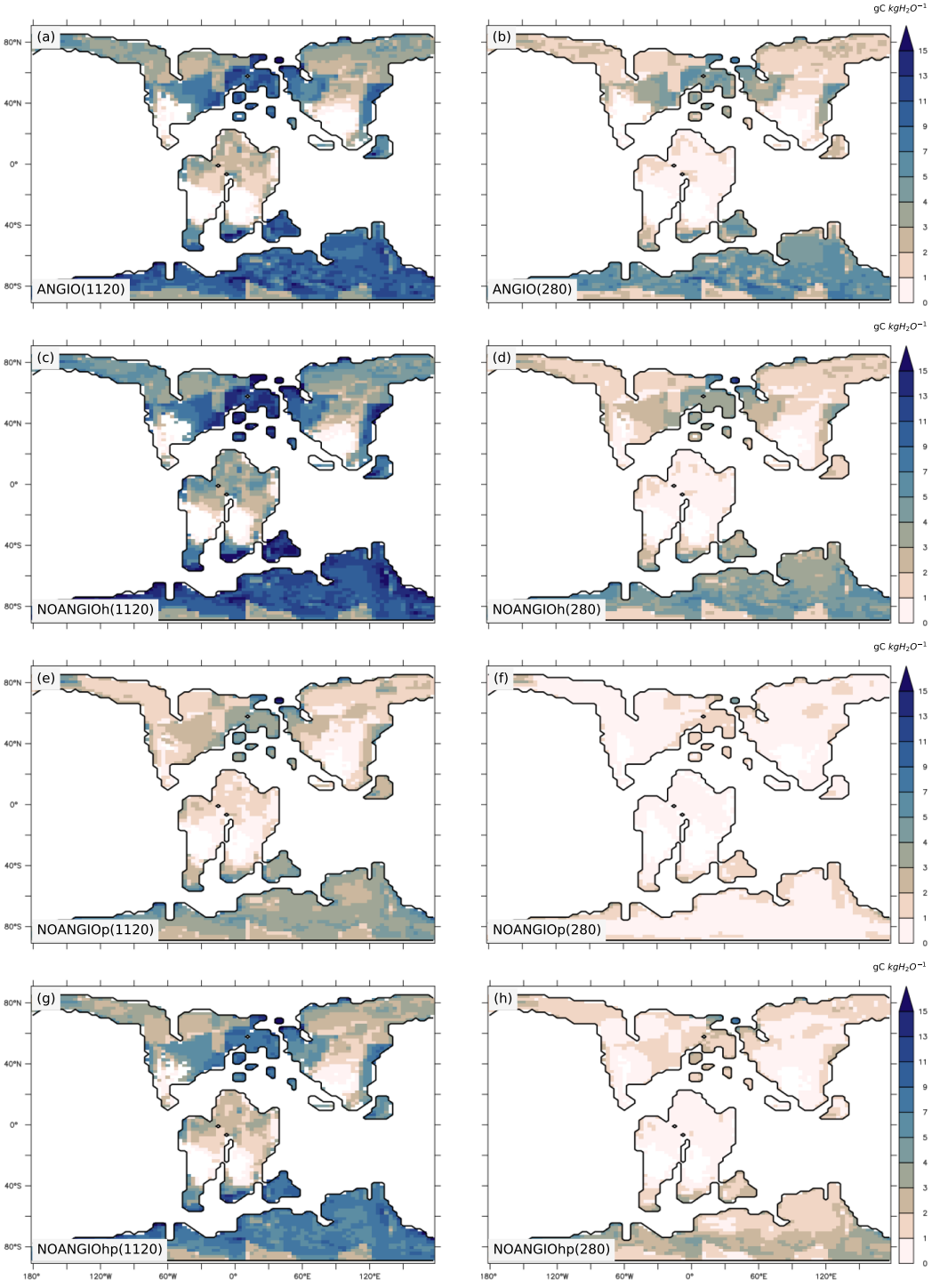

Figure 8. Annual mean WUE (gC kgH_2O^{-1}) for a) ANGIO(1120), b) ANGIO(280), c) NOANGIOh(1120), d) NOANGIOh(280), e) NOANGIOp(1120), f) NOANGIOp(280), g) NOANGIOhp(1120) and h) NOANGIOhp(280).

https://doi.org/10.5194/bg-2021-139
Preprint. Discussion started: 4 June 2021

However, at low pCO_2, WUE collapses to very low values for NOANGIOp and NOANGIOhp (Fig. 8f and h), that is driven by the large decrease in GPP when combining the low C_i to the reduction of V_{cmax} (Fig. S2f and h). Once the photosynthetic capacity is decreased, changes in GPP are the main contributor to the changes in WUE whatever the pCO_2 level prescribed.

4 Discussion

4.1 How to better account for the pre-angiosperm conductance traits in land surface models?

Fossil maximal anatomic stomatal conductance has been widely used to estimate the maximum of water flow through the stomata before and after the angiosperm radiation. Still, determining how a 5-time increase in maximal anatomic stomatal conductance translates into actual flux at the top of the canopy is challenging. We show that the complete response of the vegetation to evolving physiological and morphological traits is modulated by environmental factors such as pCO_2, light and water availability in the soil (Fig. 1).

The simplest representation of pre-angiosperm vegetation is to account for the decrease of maximal anatomic stomatal conductance by a factor of 5, consistent with the fossil records, directly by applying this factor to fcpl in the calculation of the leaf stomatal conductance (Eq. (1)). Our results show that decreasing fcpl of angiosperms at high pCO_2 does not change plant photosynthesis (Fig. 5c and S2c) but slightly decreases transpiration (Fig. 7c), driving WUE to increase (Fig. 8c) compared to the modern angiosperm prescription. Hence, a lower maximal stomatal conductance at high pCO_2 appears as an advantage compared to modern angiosperm because of a better optimization of carbon uptake over water loss. At low pCO_2, both transpiration (Fig. 7d) and photosynthesis are decreased because of the positive feedbacks of the LAI on the canopy stomatal conductance, which strengthens the initial reduction of leaf stomatal conductance compared to the modern vegetation. Despite the absence of a direct proxy for fossil plant maximum V_{cmax}, several studies have suggested to mimic the pre-angiosperm capacities by decreasing modern V_{cmax} (Boyce and Lee, 2010; Lee and Boyce, 2010), rather than fcpl, by a factor of 5. This approach is supported by our knowledge of modern plant processes that stomatal conductance interacts with assimilation in order to optimize carbon gain against water loss (Bonan, 2015) and is made possible by the coupling between stomatal conductance and photosynthetic capacity in our land-surface model (Farquhar et al., 1980; Ball et al., 1987; Krinner et al., 2005; Yin and Struik, 2009). However, applying this method leads vegetation cover to decrease at high pCO_2 (Fig. 5e and S2e) or even collapse at low pCO_2 (Fig. 5f and S2f), which is not recorded in the fossil record. As a consequence, transpiration rates (Fig. 7e and f) and WUE (Fig. 8e and f) significantly decrease at high pCO_2 and are zero at low pCO_2 compared to the modern vegetation. Hence, taking into account stomatal conductance reduction only through V_{cmax} reduction does not appear to be adequate. However, several studies suggested a decrease of V_{cmax} with increasing pCO_2 (Ainsworth and Rogers, 2007) driven by (i) a coevolution between stomatal conductance and V_{cmax} through time (Franks and Beerling, 2009a; De Boer et al., 2012) and (ii) the photosynthesis coordination theory that states that plants optimize V_{cmax} to be near the co-limitation between carboxylation rate and RuBp regeneration (Maire et al., 2012). This theory has been recently improved considering also the cost related to stomatal conductance (Stocker et al., 2020). This V_{cmax} limitation is related to the high energetic (and then respiration) cost needed to maintain a high level of Rubisco (acquisition of nitrogen). Rather than the two extreme cases that

https://doi.org/10.5194/bg-2021-139
Preprint. Discussion started: 4 June 2021


Biogeosciences Discussions Open Access EGU

decrease hydraulic or photosynthetic capacity of angiosperms by a factor of 5, we consider a covariation of fcpl and V_{cmax}, by applying half the forcing given by the fossil records (i.e. $\sqrt{1/5}$) to fcpl directly and the other half to V_{cmax}. Experimental studies on extant plant types (Lin et al., 2015) have shown differences in water-use strategy between modern angiosperm trees and gymnosperm trees. They argue that modern angiosperm trees have 2 times higher stomatal conductance sensitivity response to driving factors than gymnosperm trees, showing that our choice for fcpl*$\sqrt{1/5}$ together with V_{cmax}*$\sqrt{1/5}$ seems the most realistic. When applying this factor jointly to fcpl and V_{cmax} at a high pCO_2, our results suggest that vegetation is barely impacted, with a slight reduction of GPP (Fig. S2g), that remains enough to sustain the LAI (Fig. 5g) and a relatively high WUE (Fig. 8g) compared to the modern vegetation (Fig. 5a and 8a). Conversely at low pCO_2, LAI collapses (Fig. 5h) and GPP, transpiration and WUE reach zero (Fig. S2h, 7h and 8h) as a response to carbon assimilation drop.

At 280 ppm, sensitivity tests with a low photosynthetic capacity or together with a low hydraulic capacity can be considered as extrema where plants cannot grow (Fig. 5f and h, S2f and h) whereas experiment with modern trait vegetation corresponds to a maximum in plant productivity and transpiration (Fig. 5b, 7b and 8b). At 1120 ppm, two sets of parameters simulate a sustainable paleovegetation productivity : lowered hydraulic capacity only or lowered hydraulic and photosynthetic capacities together (Fig. 5c and g, S2c and g). However, lowering only the hydraulic capacity while keeping the high V_{cmax} as in the modern vegetation induces a nitrogen cost. Although our model does not represent the nitrogen cycle, we infer that this supplementary cost would lead to a decrease in productivity when simulating the pre-angiosperm vegetation with a modern photosynthetic capacity together with a low hydraulic capacity. Taking into account the differentiated response of vegetation to a declining pCO_2, we suggest that simultaneously decreasing fcpl and V_{cmax} by a factor of $\sqrt{1/5}$ is the most realistic representation of pre-angiosperm vegetation. The latter is consistent with previous study of Franks and Beerling (2009a) suggesting that past fluctuations in pCO_2 acted as a forcing on both V_{cmax} and stomatal conductance.

Finally, our study confirms the hypothesis that paleovegetation has evolved from a likely stage with a relatively low stomatal conductance (Fig. 4a) and V_{cmax} under high pCO_2 while sustaining high productivity (Fig. 5g, 7g and 8g) to a stage of high stomatal conductance (Fig. 4b) and V_{cmax} as in the modern vegetation, in order to preserve high productivity under low pCO_2 (Fig. 5b, 7b and 8b). The study also shows that a reasonable way to account for pre-angiosperm conductance traits is to use a model that fully describes the coupling between stomatal conductance and plant productivity from leaf to the canopy scale. Furthermore, we show that decreasing hydraulic and/or photosynthetic capacities does not coincide with a decrease of the leaf operational stomatal conductance to the same extent. Indeed, accounting for a decrease by a factor of 5, given by the maximal bound of the range expected from the maximal anatomic stomatal conductance, leaf stomatal conductance is only 3-time lower than the reference. We have a complex response because of the coupling between stomatal conductance and assimilation. While some previous studies directly decrease the transpiration rate by the factor of vein density changes from the fossil record (Boyce et al., 2009; Boyce and Lee, 2017; Boyce et al., 2010), we suggest to explicitly represent changes in hydraulic and photosynthetic capacities. Nevertheless, when embedding parallel changes on pCO_2, leaf stomatal conductance of plants with reduced hydraulic and photosynthesis capacities at high pCO_2 is nearly 6-time lower than the reference one at low pCO_2. It confirms that accounting for pCO_2 changes is mandatory to model the evolution of angiosperm leaf traits.

https://doi.org/10.5194/bg-2021-139
Preprint. Discussion started: 4 June 2021

4.2 Do the high hydraulic and photosynthetic capacities of angiosperms provide a selective advantage compared to the other plants under decreasing pCO_2?

Our work relies upon the assumption that stomata aperture maximizes carbon gain while minimizing water loss (Bonan, 2015). Both photosynthesis and stomatal conductance to H_2O are sensitive to environmental variables such as light, pCO_2 and water availability in the soil (Fig. 1). As pCO_2 has varied a lot through the Cretaceous (Fletcher et al., 2008; Wang et al., 2014), plants had to adjust their stomatal conductance. Our study suggests that having a high stomatal conductance, which means a large vein density and a high V_{cmax}, provides little advantage compared to a low stomatal conductance under high pCO_2. In contrast, having a high stomatal conductance under low pCO_2 may confer a competitive advantage over plants with limited stomatal conductance to assimilate carbon. But this higher stomatal conductance should be linked to an increase in V_{cmax} to sustain growth. In that sense, fossil records provide evidence of plant traits evolution during the angiosperm radiation. Fossils of basal angiosperms show that vein density was as low as the other plant types because having a high vein density under high pCO_2 was not necessary for the plants to grow. Then, the pCO_2 likely declined (Fletcher et al., 2008; Wang et al., 2014). At that time, we confirm the hypothesis that angiosperms evolved towards leaves more and more densely irrigated together with a more efficient biochemistry that allowed them to have an increasingly stomatal conductance and photosynthetic capacity to counteract the effect of pCO_2 decrease on carbon assimilation. Among others, this evolution of physiological leaves traits has given a competitive advantage to angiosperms compared to gymnosperms dominating the vegetation of the period to colonize almost all the terrestrial ecosystems. Our results are consistent with that of Franks and Beerling (2009a), which have shown that WUE co-evolves positively with variations in pCO_2 over the Phanerozoic : periods with high pCO_2 strengthen GPP, meanwhile a potential decrease of transpiration rate by the closing of the stomata. They also show that even after the evolution of angiosperm leaf morphology and biochemistry, WUE is estimated to have been at its lowest level since the Carboniferous. Our model consistently represents the range of WUE deducted by Franks and Beerling (2009a) under different pCO_2 : between 5 and 9 gC kgH_2O^{-1} (Fig. 8a and b). Moreover, there is a likely co-adaptation of stomatal traits and leaf venation which implies a better optimisation of carbon gain against water loss (De Boer et al., 2012). Progressively, under decreasing pCO_2, angiosperms with high stomatal density and low stomatal size (Franks and Beerling, 2009a, b) likely invested increasingly energy in building more and more veins to sustain the higher stomatal conductance and then carbon assimilation, while other plants did not. The innovation of angiosperms in densely water transport networks could have become a necessity to support higher stomatal conductance and prevent plant desiccation (De Boer et al., 2012).

4.3 What are the limitations of our modelling choices?

As a first step toward understanding the impact of trait evolution on the hydraulic and photosynthetic capacities of angiosperms, we have chosen to simulate the Aptian (115 Ma) because this time period corresponds to the first step of increasing vein density found in the fossil record (Feild et al., 2011a). To get an exhaustive view of the angiosperm evolution, future studies will benefit from considering similar experiments with boundary conditions set several million years before and after the Aptian. Specifically, exploring cold and warm extremes of the Cretaceous, such as the Cenomanian-Turonian (95 Ma) and the Maastrichtian

https://doi.org/10.5194/bg-2021-139
Preprint. Discussion started: 4 June 2021

(70 Ma) would be valuable, as climate and pCO_2 have been shown to vary a lot during these periods (Ladant and Donnadieu, 2016).

The vegetation map we used (Fig. 3) results from two efforts of (i) compilation and spatialization of the Aptian paleobotanical records (Sewall et al., 2007) and (ii) conversion of the fossil data into plant functional types combination (Table S1). Each of these two steps include uncertainties that can propagate into our results, but can be hardly quantified. We acknowledge that the prescribed vegetation cover, especially in the tropics, can potentially alter the radiative balance and the hydrological cycle (e.g., Port et al., 2016). It is however unlikely that the Aptian vegetation cover would be very different from the one provided by Sewall et al. (2007), given the compilation effort made for this reconstruction. Further studies could still circumvent this potential issue by running a fully dynamical vegetation model, i.e. by allowing PFTs to spatially settle in regions where the simulated climate is the most appropriate.

Recent studies about Paleozoic vegetation transitions indicate that differences in transpiration rates also arise from the ratio of carbon over nitrogen (White et al., 2020; Richey et al., 2021). As mentioned earlier, the ORCHIDEE version we used does not explicitly represent the nitrogen cycle, preventing us from considering the additional cost to maintain high photosynthetic capacity with lower hydraulic capacity. The recent developments of a new version of ORCHIDEE that does include the nitrogen cycle (Vuichard et al., 2019) will help to account for this process, provided that good constraints can be obtained regarding the C:N ratio of Cretaceous vegetation and soils.

Through the use of the coupled LMDZ and ORCHIDEE models, our approach includes the pivotal coupling between atmosphere and vegetation. However by using fixed sea-surface temperatures, we neglect the feedbacks from the ocean-atmosphere coupling that could occur as a response to simulated changes in vegetation cover. Although sensitivity experiments with strong changes in vegetation suggested ocean feedbacks could play a significant role on the continental hydrological cycle (Davin and de Noblet-Ducoudré, 2010), our choice was motivated by (i) the will to focus on first-order continental processes, (ii) the computing cost required to equilibrate fully coupled simulations that typically require more than 3000 simulated years (Sepulchre et al., 2020), the fact that comparable studies either used fixed-SSTs (Boyce and Lee, 2010; Lee and Boyce, 2010) or slab oceans (White et al., 2020).

Finally our parameterization of stomatal conductance in ORCHIDEE from Yin and Struik (2009) (Eq. (1)) is semi-empirical. A refinement of our modelling approach would be to use a stomatal conductance model based on optimisation theory, that explicitly describes the stomata functioning so as to optimise carbon gain against water loss (Medlyn et al., 2011; Buckley and Mott, 2013; Buckley, 2017). In particular, the model we use here simply links external forcing to leaf stomatal conductance by an empirical term of coupling fcpl that describe all the processes related to stomatal conductance. The α factor applied in Eq. (1) to the coupling factor (fcpl) does not fully represent the change in the maximal anatomic stomatal conductance as it should be considering changes in vein density (stomatal density and size). It emphasizes the need, in the future, to improve the parameterization of stomatal conductance in global mode by explicitly modelling both structural and dynamic conductance.

https://doi.org/10.5194/bg-2021-139
Preprint. Discussion started: 4 June 2021


Biogeosciences Discussions Open Access EGU

5 Conclusions

In line with recent studies focusing on Paleozoic vegetation transitions (White et al., 2020; Richey et al., 2021), the purpose of our study is to better represent past vegetation in earth system models by implementing "paleo-traits" in the vegetation parameterizations. Our approach involves an atmosphere-vegetation model, which couples stomatal conductance and carbon assimilation, with an ecophysiological model based on angiosperm fossil records. Here, it allows us to evaluate three different paleovegetation prescriptions under two end-member scenarios of pCO_2 for the Cretaceous. We show that the simulated vegetation cover, transpiration rate and water use efficiency are sensitive to the paleovegetation trait prescribed. Only accounting for hydraulic capacity reduction provides no significant change in LAI, GPP and transpiration, while slightly increasing WUE at high pCO_2. In contrast, global transpiration decreases at low pCO_2 because of the positive feedback between LAI and stomatal conductance. On the other hand, only accounting for photosynthetic capacity reduction gives a substantial decrease or even a collapse of vegetation at high or low pCO_2 respectively, which is not recorded in the fossil. Combining a reduction of hydraulic capacity with that of photosynthetic capacity does not affect the plant productivity and LAI at high pCO_2 while vegetation collapses at low pCO_2. All the results taken together demonstrate that under high pCO_2 the reduced stomatal conductance of the pre-angiosperm vegetation is not a limiting factor on productivity. It also shows that high values of V_{cmax} as observed in modern angiosperms do not enhance plant productivity, whereas maintaining the high V_{cmax} likely requires higher leaf nitrogen concentration and higher energy demand. Therefore, the combining decrease of hydraulic and photosynthetic capacities seems the most realistic physiological parameterization for pre-angiosperms in the specific high pCO_2 context of the Cretaceous. This is supported by evidence of coevolution inferred from previous studies (Franks and Beerling, 2009a, b) and the ratio of stomatal conductance between modern angiosperms and gymnosperms from in-situ experiments (Lin et al., 2015). This result is also consistent with recent studies on coordination theory (Maire et al., 2012; Stocker et al., 2020).

Our study also suggests that pre-angiosperm vegetation with low hydraulic and photosynthetic capacities was adapted to high pCO_2 by sustaining productivity and a high WUE. Conversely, it was not adapted to lower pCO_2 as GPP collapses. Modelling the full coupling between GPP and stomatal conductance allows to understand why increasing both structural conductance and maximum photosynthetic capacity, even at an expense of a possible increasing water loss, was a selective advantage with decreasing pCO_2 and is the likely explanation for observed increasing structural conductance of angiosperms since the Cretaceous, consistent with previous studies (Franks and Beerling, 2009a, b; Boyce and Zwieniecki, 2012; Brodribb and Feild, 2010). From a low stomatal conductance (low vein density and V_{cmax}) similar to that of gymnosperms under high pCO_2, angiosperms evolve towards a high stomatal conductance (high vein density and V_{cmax}) to counteract the effect of the pCO_2 decrease on carbon assimilation.

While this study provides clues on how to account for angiosperm evolutionary traits in paleoclimate simulations, further work is needed to assess the potential climate effects of the Cretaceous angiosperm leaf evolution, especially on the hydrological cycle and the energy balance at the land surface. Furthermore, allowing dynamic vegetation would be an important future refinement of this research to model feedbacks between vegetation and climate. With such a model, we may question the veracity of the reciprocity with the human-induced increase in pCO_2. Building leaves with high vein density and V_{cmax} induces

https://doi.org/10.5194/bg-2021-139
Preprint. Discussion started: 4 June 2021

an investment in nutrients and energy that could be an extra cost for plants without benefit under a higher pCO_2. That would suggest that plants should evolve back to a reduced stomatal conductance and V_{cmax}. However, the pace of the current increase in pCO_2 is dramatically higher than the million-year time scale of Cretaceous changes, and likely incompatible with a genetic plant adaptation. Whether extant plants will be able to adjust their physiological and morphological traits or not to the human perturbation is a challenging question for future studies.

Data availability. We provide the simulation outputs in the online repository : http://doi.org/10.5281/zenodo.4773541

Author contributions. JB, PS, NVIO and NVUI designed the work. Under supervision of PS, NVIO and NVUI, JB performed the simulations, processed the data, wrote the manuscript and drew the figures, except Fig. 1 drawn by PS. All authors reviewed and approved the manuscript.

Competing interests. The authors declare that they have no conflict of interest.

Acknowledgements. This work was granted access to the HPC resources of TGCC under allocation 2019-A0090102212 made by GENCI. JB, NVIO and NVUI are supported by the *Commisariat à l'énergie atomique et aux énergies alternatives* (CEA). PS is supported by *Centre national de la recherche scientifique* (CNRS).

https://doi.org/10.5194/bg-2021-139
Preprint. Discussion started: 4 June 2021

References

Ainsworth, E. A. and Rogers, A.: The response of photosynthesis and stomatal conductance to rising [CO2]: mechanisms and environmental interactions, Plant Cell Environ., 30, 258–270, https://doi.org/https://doi.org/10.1111/j.1365-3040.2007.01641.x, 2007.

Ball, J. T., Woodrow, I. E., and Berry, J. A.: A model predicting stomatal conductance and its contribution to the control of photosynthesis under different environmental conditions, in: Progress in photosynthesis research, pp. 221–224, Springer, https://doi.org/https://doi.org/10.1007/978-94-017-0519-6_48, 1987.

Bathiany, S., Claussen, M., Brovkin, V., Raddatz, T., and Gayler, V.: Combined biogeophysical and biogeochemical effects of large-scale forest cover changes in the MPI earth system model, Biogeosciences, 7, 1383–1399, https://doi.org/https://doi.org/10.5194/bg-7-1383-2010, 2010.

Betts, R. A., Cox, P. M., Lee, S. E., and Woodward, F. I.: Contrasting physiological and structural vegetation feedbacks in climate change simulations, Nature, 387, 796–799, https://doi.org/https://doi-org.insu.bib.cnrs.fr/10.1038/42924, 1997.

Bonan, G.: Ecological climatology: concepts and applications, Cambridge University Press, 2015.

Boyce, C. K. and Lee, J.-E.: An exceptional role for flowering plant physiology in the expansion of tropical rainforests and biodiversity, P. Roy. Soc. B-Biol. Sci., 277, 3437–3443, https://doi.org/https://doi.org/10.1098/rspb.2010.0485, 2010.

Boyce, C. K. and Lee, J.-E.: Plant evolution and climate over geological timescales, Annu. Rev. Earth Pl. Sc., 45, 61–87, https://doi.org/https://doi.org/10.1146/annurev-earth-063016-015629, 2017.

Boyce, C. K. and Zwieniecki, M. A.: Leaf fossil record suggests limited influence of atmospheric CO2 on terrestrial productivity prior to angiosperm evolution, P. Natl. Acad. Sci. USA, 109, 10 403–10 408, https://doi.org/https://doi.org/10.1073/pnas.1203769109, 2012.

Boyce, C. K., Brodribb, T. J., Feild, T. S., and Zwieniecki, M. A.: Angiosperm leaf vein evolution was physiologically and environmentally transformative, P. Roy. Soc. B-Biol. Sci., 276, 1771–1776, https://doi.org/https://doi.org/10.1098/rspb.2008.1919, 2009.

Boyce, C. K., Lee, J.-E., Feild, T. S., Brodribb, T. J., and Zwieniecki, M. A.: Angiosperms Helped Put the Rain in the Rainforests: The Impact of Plant Physiological Evolution on Tropical Biodiversity1, Ann. Mo. Bot. Gard., 97, 527–540, https://doi.org/https://doi.org/10.3417/2009143, 2010.

Braconnot, P., Joussaume, S., Marti, O., and De Noblet, N.: Synergistic feedbacks from ocean and vegetation on the African monsoon response to mid-Holocene insolation, Geophys. Res. Lett., 26, 2481–2484, https://doi.org/https://doi.org/10.1029/1999GL006047, 1999.

Brodribb, T. J. and Feild, T. S.: Leaf hydraulic evolution led a surge in leaf photosynthetic capacity during early angiosperm diversification, Ecol. Lett., 13, 175–183, https://doi.org/https://doi.org/10.1111/j.1461-0248.2009.01410.x, 2010.

Brodribb, T. J., Feild, T. S., and Jordan, G. J.: Leaf maximum photosynthetic rate and venation are linked by hydraulics, Plant Physiol., 144, 1890–1898, https://doi.org/https://doi.org/10.1104/pp.107.101352, 2007.

Brovkin, V., Claussen, M., Driesschaert, E., Fichefet, T., Kicklighter, D., Loutre, M.-F., Matthews, H. D., Ramankutty, N., Schaeffer, M., and Sokolov, A.: Biogeophysical effects of historical land cover changes simulated by six Earth system models of intermediate complexity, Clim. Dynam., 26, 587–600, https://doi.org/https://doi.org/10.1007/s00382-005-0092-6, 2006.

Brovkin, V., Raddatz, T., Reick, C. H., Claussen, M., and Gayler, V.: Global biogeophysical interactions between forest and climate, Geophys. Res. Lett., 36, https://doi.org/https://doi.org/10.1029/2009GL037543, 2009.

Buckley, T. N.: Modeling stomatal conductance, Plant physiology, 174, 572–582, https://doi.org/https://doi.org/10.1104/pp.16.01772, 2017.

Buckley, T. N. and Mott, K. A.: Modelling stomatal conductance in response to environmental factors, Plant, cell & environment, 36, 1691–1699, https://doi.org/https://doi.org/10.1111/pce.12140, 2013.

https://doi.org/10.5194/bg-2021-139
Preprint. Discussion started: 4 June 2021

Charney, J., Stone, P. H., and Quirk, W. J.: Drought in the Sahara: a biogeophysical feedback mechanism, Science, 187, 434–435, https://doi.org/https://doi.org/10.1126/science.187.4175.434, 1975.

Christenhusz, M. J. and Byng, J. W.: The number of known plants species in the world and its annual increase, Phytotaxa, 261, 201–217, https://doi.org/https://doi.org/10.11646/phytotaxa.261.3.1, 2016.

Condamine, F. L., Silvestro, D., Koppelhus, E. B., and Antonelli, A.: The rise of angiosperms pushed conifers to decline during global cooling, P. Natl. Acad. Sci. USA, 117, 28 867–28 875, https://doi.org/https://doi.org/10.1073/pnas.2005571117, 2020.

Davin, E. L. and de Noblet-Ducoudré, N.: Climatic impact of global-scale deforestation: Radiative versus nonradiative processes, J. Climate, 23, 97–112, https://doi.org/https://doi.org/10.1175/2009JCLI3102.1, 2010.

De Boer, H. J., Eppinga, M. B., Wassen, M. J., and Dekker, S. C.: A critical transition in leaf evolution facilitated the Cretaceous angiosperm revolution, Nat. Commun., 3, 1–11, https://doi.org/https://doi-org.insu.bib.cnrs.fr/10.1038, 2012.

Dow, G. J. and Bergmann, D. C.: Patterning and processes: how stomatal development defines physiological potential, Curr. Opin. Plant Biol., 21, 67–74, https://doi.org/https://doi.org/10.1016/j.pbi.2014.06.007, 2014.

Dow, G. J., Bergmann, D. C., and Berry, J. A.: An integrated model of stomatal development and leaf physiology, New Phytol., 201, 1218–1226, https://doi.org/https://doi.org/10.1111/nph.12608, 2014.

Ducoudré, N. I., Laval, K., and Perrier, A.: SECHIBA, a new set of parameterizations of the hydrologic exchanges at the land-atmosphere interface within the LMD atmospheric general circulation model, J. Climate, 6, 248–273, https://doi.org/https://doi.org/10.1175/1520-0442(1993)006<0248:SANSOP>2.0.CO;2, 1993.

Dury, M., Mertens, L., Fayolle, A., Verbeeck, H., Hambuckers, A., and François, L.: Refining species traits in a dynamic vegetation model to project the impacts of climate change on tropical trees in Central Africa, Forests, 9, 722, https://doi.org/https://doi.org/10.3390/f9110722, 2018.

Farquhar, G. D., von Caemmerer, S. v., and Berry, J. A.: A biochemical model of photosynthetic CO 2 assimilation in leaves of C 3 species, Planta, 149, 78–90, https://doi.org/https://doi.org/10.1007/BF00386231, 1980.

Feild, T. S., Brodribb, T. J., Iglesias, A., Chatelet, D. S., Baresch, A., Upchurch, G. R., Gomez, B., Mohr, B. A., Coiffard, C., Kvacek, J., et al.: Fossil evidence for Cretaceous escalation in angiosperm leaf vein evolution, P. Natl. Acad. Sci. USA, 108, 8363–8366, https://doi.org/https://doi.org/10.1073/pnas.1014456108, 2011a.

Feild, T. S., Upchurch, G. R., Chatelet, D. S., Brodribb, T. J., Grubbs, K. C., Samain, M.-S., and Wanke, S.: Fossil evidence for low gas exchange capacities for Early Cretaceous angiosperm leavesEarly Angiosperm Leaf Gas Exchange, Paleobiology, 37, 195–213, https://doi.org/https://doi.org/10.1666/10015.1, 2011b.

Fisher, R. A. and Koven, C. D.: Perspectives on the future of land surface models and the challenges of representing complex terrestrial systems, J. Adv. Model. Earth Sy., 12, e2018MS001 453, https://doi.org/https://doi.org/10.1029/2018MS001453, 2020.

Fletcher, B. J., Brentnall, S. J., Anderson, C. W., Berner, R. A., and Beerling, D. J.: Atmospheric carbon dioxide linked with Mesozoic and early Cenozoic climate change, Nat. Geosci., 1, 43, https://doi.org/https://doi-org.insu.bib.cnrs.fr/10.1038/ngeo.2007.29, 2008.

Fraedrich, K., Kleidon, A., and Lunkeit, F.: A green planet versus a desert world: Estimating the effect of vegetation extremes on the atmosphere, J. Climate, 12, 3156–3163, https://doi.org/https://doi.org/10.1175/1520-0442(1999)012<3156:AGPVAD>2.0.CO;2, 1999.

Franks, P. and Beerling, D.: CO2-forced evolution of plant gas exchange capacity and water-use efficiency over the Phanerozoic, Geobiology, 7, 227–236, https://doi.org/https://doi.org/10.1111/j.1472-4669.2009.00193.x, 2009a.

Franks, P. J. and Beerling, D. J.: Maximum leaf conductance driven by CO2 effects on stomatal size and density over geologic time, P. Natl. Acad. Sci. USA, 106, 10 343–10 347, https://doi.org/https://doi.org/10.1073/pnas.0904209106, 2009b.

https://doi.org/10.5194/bg-2021-139
Preprint. Discussion started: 4 June 2021

Franks, P. J. and Farquhar, G. D.: The effect of exogenous abscisic acid on stomatal development, stomatal mechanics, and leaf gas exchange in Tradescantia virginiana, Plant Physiol., 125, 935–942, https://doi.org/https://doi.org/10.1104/pp.125.2.935, 2001.

Gibbard, S., Caldeira, K., Bala, G., Phillips, T. J., and Wickett, M.: Climate effects of global land cover change, Geophys. Res. Lett., 32, https://doi.org/https://doi.org/10.1029/2005GL024550, 2005.

Hourdin, F., Foujols, M.-A., Codron, F., Guemas, V., Dufresne, J.-L., Bony, S., Denvil, S., Guez, L., Lott, F., Ghattas, J., et al.: Impact of the LMDZ atmospheric grid configuration on the climate and sensitivity of the IPSL-CM5A coupled model, Clim. Dynam., 40, 2167–2192, https://doi.org/https://doi.org/10.1007/s00382-012-1411-3, 2013.

Jarvis, A., Mansfield, T., and Davies, W. J.: Stomatal behaviour, photosynthesis and transpiration under rising CO2, Plant Cell Environ., 22, 639–648, https://doi.org/https://doi.org/10.1046/j.1365-3040.1999.00407.x, 1999.

Kattge, J. and Knorr, W.: Temperature acclimation in a biochemical model of photosynthesis: a reanalysis of data from 36 species, Plant Cell Environ., 30, 1176–1190, https://doi.org/https://doi.org/10.1111/j.1365-3040.2007.01690.x, 2007.

Kattge, J., Bönisch, G., Díaz, S., Lavorel, S., Prentice, I. C., Leadley, P., Tautenhahn, S., Werner, G. D., Aakala, T., Abedi, M., et al.: TRY plant trait database–enhanced coverage and open access, Glob. Change Biol, 26, 119–188, https://doi.org/https://doi.org/10.1111/gcb.14904, 2020.

Kleidon, A., Fraedrich, K., and Heimann, M.: A green planet versus a desert world: Estimating the maximum effect of vegetation on the land surface climate, Climatic Change, 44, 471–493, https://doi.org/https://doi.org/10.1023/A:1005559518889, 2000.

Krinner, G., Viovy, N., de Noblet-Ducoudré, N., Ogée, J., Polcher, J., Friedlingstein, P., Ciais, P., Sitch, S., and Prentice, I. C.: A dynamic global vegetation model for studies of the coupled atmosphere-biosphere system, Global Biogeochem. Cy., 19, https://doi.org/https://doi.org/10.1029/2003GB002199, 2005.

Ladant, J.-B. and Donnadieu, Y.: Palaeogeographic regulation of glacial events during the Cretaceous supergreenhouse, Nat. Commun., 7, 1–9, https://doi.org/https://doi.org/10.1038/ncomms12771, 2016.

Lee, J.-E. and Boyce, K.: Impact of the hydraulic capacity of plants on water and carbon fluxes in tropical South America, J. Geophys. Res.-Atmos., 115, https://doi.org/https://doi.org/10.1029/2010JD014568, 2010.

Leuning, R., Kelliher, F. M., De Pury, D., and Schulze, E.-D.: Leaf nitrogen, photosynthesis, conductance and transpiration: scaling from leaves to canopies, Plant Cell Environ., 18, 1183–1200, https://doi.org/https://doi.org/10.1111/j.1365-3040.1995.tb00628.x, 1995.

Lin, Y.-S., Medlyn, B. E., Duursma, R. A., Prentice, I. C., Wang, H., Baig, S., Eamus, D., De Dios, V. R., Mitchell, P., Ellsworth, D. S., et al.: Optimal stomatal behaviour around the world, Nat. Clim. Change, 5, 459–464, https://doi.org/https://doi-org.insu.bib.cnrs.fr/10.1038/nclimate2550, 2015.

Maire, V., Martre, P., Kattge, J., Gastal, F., Esser, G., Fontaine, S., and Soussana, J.-F.: The coordination of leaf photosynthesis links C and N fluxes in C 3 plant species, PloS one, 7, e38 345, https://doi.org/https://doi.org/10.1371/journal.pone.0038345, 2012.

McElwain, J. C., Yiotis, C., and Lawson, T.: Using modern plant trait relationships between observed and theoretical maximum stomatal conductance and vein density to examine patterns of plant macroevolution, New Phytol., 209, 94–103, https://doi.org/https://doi.org/10.1111/nph.13579, 2016.

Medlyn, B. E., Duursma, R. A., Eamus, D., Ellsworth, D. S., Prentice, I. C., Barton, C. V., Crous, K. Y., De Angelis, P., Freeman, M., and Wingate, L.: Reconciling the optimal and empirical approaches to modelling stomatal conductance, Global Change Biology, 17, 2134–2144, https://doi.org/https://doi.org/10.1111/j.1365-2486.2010.02375.x, 2011.

Peng, S.-S., YUE, C., and CHANG, J.-F.: Developments and applications of terrestrial biosphere model, Chinese Journal of Plant Ecology, 44, 436, https://doi.org/https://doi.org/10.17521/cjpe.2019.0315, 2020.

Port, U., Claussen, M., and Brovkin, V.: Radiative forcing and feedback by forests in warm climates–a sensitivity study, Earth Syst. Dynam., 7, 535–547, https://doi.org/https://doi.org/10.5194/esd-7-535-2016, 2016.

Richey, J. D., Montañez, I. P., White, J. D., DiMichele, W. A., Matthaeus, W. J., Poulsen, C. J., Macarewich, S. I., and Looy, C. V.: Modeled physiological mechanisms for observed changes in the late Paleozoic plant fossil record, Palaeogeogr. Palaeocl., 562, 110 056, https://doi.org/https://doi.org/10.1016/j.palaeo.2020.110056, 2021.

Rosnay, P. d. and Polcher, J.: Modelling root water uptake in a complex land surface scheme coupled to a GCM, Hydrol. Earth Syst. Sc., 2, 239–255, https://doi.org/https://doi.org/10.5194/hess-2-239-1998, 1998.

Scheiter, S., Langan, L., and Higgins, S. I.: Next-generation dynamic global vegetation models: learning from community ecology, New Phytol., 198, 957–969, https://doi.org/https://doi.org/10.1111/nph.12210, 2013.

Sepulchre, P., Caubel, A., Ladant, J.-B., Bopp, L., Boucher, O., Braconnot, P., Brockmann, P., Cozic, A., Donnadieu, Y., Dufresne, J.-L., et al.: IPSL-CM5A2–an Earth system model designed for multi-millennial climate simulations, Geosci. Model Dev., 13, 3011–3053, https://doi.org/https://doi.org/10.5194/gmd-13-3011-2020, 2020.

Sewall, J. v., Van De Wal, R., Zwan, K. v., Oosterhout, C. v., Dijkstra, H., and Scotese, C.: Climate model boundary conditions for four Cretaceous time slices, Clim. Past, 3, 647–657, https://doi.org/https://doi.org/10.5194/cp-3-647-2007, 2007.

Sitch, S., Smith, B., Prentice, I. C., Arneth, A., Bondeau, A., Cramer, W., Kaplan, J. O., Levis, S., Lucht, W., Sykes, M. T., et al.: Evaluation of ecosystem dynamics, plant geography and terrestrial carbon cycling in the LPJ dynamic global vegetation model, Glob. Change Biol., 9, 161–185, https://doi.org/https://doi.org/10.1046/j.1365-2486.2003.00569.x, 2003.

Stocker, B. D., Wang, H., Smith, N. G., Harrison, S. P., Keenan, T. F., Sandoval, D., Davis, T., and Prentice, I. C.: P-model v1. 0: an optimality-based light use efficiency model for simulating ecosystem gross primary production, Geosci. Model Dev., 13, 1545–1581, https://doi.org/https://doi.org/10.5194/gmd-13-1545-2020, 2020.

Sun, X. and Barros, A. P.: Impact of Amazonian evapotranspiration on moisture transport and convection along the eastern flanks of the tropical Andes, Q. J. Roy. Meteor. Soc., 141, 3325–3343, https://doi.org/https://doi.org/10.1002/qj.2615, 2015.

Vuichard, N., Messina, P., Luyssaert, S., Guenet, B., Zaehle, S., Ghattas, J., Bastrikov, V., and Peylin, P.: Accounting for carbon and nitrogen interactions in the global terrestrial ecosystem model ORCHIDEE (trunk version, rev 4999): multi-scale evaluation of gross primary production, Geosci. Model Dev., 12, 4751–4779, https://doi.org/https://doi.org/10.5194/gmd-12-4751-2019, 2019.

Wang, Y., Huang, C., Sun, B., Quan, C., Wu, J., and Lin, Z.: Paleo-CO2 variation trends and the Cretaceous greenhouse climate, Earth-Sci. Rev., 129, 136–147, https://doi.org/https://doi.org/10.1016/j.earscirev.2013.11.001, 2014.

White, J. D., Montañez, I. P., Wilson, J. P., Poulsen, C. J., McElwain, J. C., DiMichele, W. A., Hren, M. T., Macarewich, S., Richey, J. D., and Matthaeus, W. J.: A process-based ecosystem model (Paleo-BGC) to simulate the dynamic response of Late Carboniferous plants to elevated O2 and aridification, Am. J. Sci., 320, 547–598, https://doi.org/https://doi.org/10.2475/09.2020.01, 2020.

Yin, X. and Struik, P.: C3 and C4 photosynthesis models: An overview from the perspective of crop modelling, NJAS-Wagen. J. Life Sc., 57, 27–38, https://doi.org/https://doi.org/10.1016/j.njas.2009.07.001, 2009.